Redox Biology 26 (2019) 101273

Contents lists available at ScienceDirect

Redox Biology

journal homepage: www.elsevier.com/locate/redox

Research Paper

A novel NOX2 inhibitor attenuates human neutrophil oxidative stress and ameliorates inflammatory arthritis in mice

Fu-Chao Liu[a,b,1], Huang-Ping Yu[a,b,1], Po-Jen Chen[c,d,1], Hsuan-Wu Yang[d,1], Shih-Hsin Chang[d,e], Cherng-Chyi Tzeng[f,g], Wei-Jen Cheng[h,i], You-Ren Chen[f,g], Yeh-Long Chen[f,g,*], Tsong-Long Hwang[b,d,e,j,k,**]

[a] College of Medicine, Chang Gung University, Taoyuan, 333, Taiwan
[b] Department of Anesthesiology, Chang Gung Memorial Hospital, Taoyuan, 333, Taiwan
[c] Department of Cosmetic Science, Providence University, Taichung, 433, Taiwan
[d] Graduate Institute of Natural Products, College of Medicine, Chang Gung University, Taoyuan, 333, Taiwan
[e] Research Center for Chinese Herbal Medicine, Research Center for Food and Cosmetic Safety, and Graduate Institute of Health Industry Technology, College of Human Ecology, Chang Gung University of Science and Technology, Taoyuan, 333, Taiwan
[f] Department of Medicinal and Applied Chemistry, College of Life Science, Kaohsiung Medical University, Kaohsiung, 807, Taiwan
[g] Department of Medical Research, Kaohsiung Medical University-Hospital, Kaohsiung, 807, Taiwan
[h] Graduate Institute of Clinical Medicine, College of Medicine, Chang Gung University, Taoyuan, 333, Taiwan
[i] Department of Traditional Chinese Medicine, Center of Traditional Chinese Medicine, Chang Gung Memorial Hospital, Taoyuan, 333, Taiwan
[j] Chinese Herbal Medicine Research Team, Healthy Aging Research Center, Chang Gung University, Taoyuan, 333, Taiwan
[k] Department of Chemical Engineering, Ming Chi University of Technology, New Taipei City, 243, Taiwan

ARTICLE INFO

Keywords:
Inflammatory arthritis
CYR5099
NADPH oxidase 2
Neutrophil
Reactive oxygen species

ABSTRACT

Neutrophil infiltration plays a significant pathological role in inflammatory diseases. NADPH oxidase type 2 (NOX2) is a respiratory burst oxidase that generates large amounts of superoxide anion ($O_2^{\bullet-}$) and subsequent other reactive oxygen species (ROS). NOX2 is an emerging therapeutic target for treating neutrophilic inflammatory diseases. Herein, we show that 4-[(4-(dimethylamino)butoxy)imino]-1-methyl-1*H*-benzo[*f*]indol-9(4*H*)-one (CYR5099) acts as a NOX2 inhibitor and exerts a protective effect against complete Freund's adjuvant (CFA)-induced inflammatory arthritis in mice. CYR5099 restricted the production of $O_2^{\bullet-}$ and ROS, but not the elastase release, in human neutrophils activated with various stimulators. The upstream signaling pathways of NOX2 were not inhibited by CYR5099. Significantly, CYR5099 inhibited NOX2 activity in activated human neutrophils and in reconstituted subcellular assays. In addition, CYR5099 reduced ROS production, neutrophil infiltration, and edema in CFA-induced arthritis in mice. Our findings suggest that CYR5099 is a NOX2 inhibitor and has therapeutic potential for treating neutrophil-dominant oxidative inflammatory disorders.

1. Introduction

Leukocytes are major immune cells in the human circulatory system. Neutrophils are the predominant leukocytes for defense against pathogen invasion [1,2]. However, neutrophils phagocytose pathogens and generate cytotoxic mediators that induce severe inflammatory responses [1,3]. Overproduction of superoxide anion ($O_2^{\bullet-}$), a reactive oxygen species (ROS) precursor, from neutrophils can damage surrounding cells and result in inflammatory disorders and autoimmune diseases [3–5].

NADPH oxidase type 2 (NOX2) is composed of six subunits and responsible for $O_2^{\bullet-}$ generation during respiratory burst. With stimulation, membrane-associated catalytic subunit, $gp91^{phox}$, assembles with other subunits, $p22^{phox}$, $p47^{phox}$, $p67^{phox}$, $p40^{phox}$, and Rac2, to form active NADPH oxidase in neutrophils [5,6]. Prolonged and uncontrolled ROS generation by NOX2 is a crucial pathogenic factor in the pathogenesis of several inflammatory disorders and autoimmune diseases, such as arthritis, acute respiratory distress syndrome, or systemic lupus erythematosus [3,7–9]. Importantly, pharmacological inhibition or deficiency of NOX2 can restrict inflammatory responses and

* Corresponding author. Department of Medicinal and Applied Chemistry, College of Life Science, Kaohsiung Medical University, Kaohsiung, 807, Taiwan.
** Corresponding author. Graduate Institute of Natural Products, College of Medicine, Chang Gung University, Taoyuan, 333, Taiwan.
E-mail addresses: yeloch@kmu.edu.tw (Y.-L. Chen), htl@mail.cgu.edu.tw (T.-L. Hwang).
[1] These authors contributed equally to this work.

https://doi.org/10.1016/j.redox.2019.101273
Received 5 June 2019; Received in revised form 4 July 2019; Accepted 9 July 2019
Available online 10 July 2019

Abbreviations

ABTS	2,2′-azino-bis(3-ethylbenzothiazoline-6-sulphonic acid)
CB	cytochalasin B
CFA	complete Freund's adjuvant
CYR5099	(4-[(4-(dimethylamino)butoxy)imino]-1-methyl-1*H*-benzo[*f*]indol-9(4*H*)-one)
DPI	diphenyleneiodonium
ERK	extracellular signal-regulated kinase
fMLF	*N*-formyl-L-methionyl-L-leucyl-L-phenylalanine
f-MMYALF	*N*-formyl-Met-Met-Tyr-Ala-Leu-Phe
FPR	formyl peptide receptor
GPCR	G protein-couple receptor
IC_{50}	The half maximal inhibitory concentration
JNK	c-Jun *N*-terminal kinase
LDH	lactate dehydrogenase
LPS	lipopolysaccharide
m-3M3FBS	2,4,6-trimethyl-*N*-(meta-3-trifluoromethyl-phenyl)-benzenesulfonamide
MAPK	mitogen-activated protein kinase
MMK1	Leu-Glu-Ser-Ile-Phe-Arg-Ser-Leu-Leu-Phe-Arg-Val-Met
MPO	myeloperoxidase
NOX2	NADPH oxidase type 2
PKC	protein kinase C
PMA	phorbol-12-myristate-13-acetate
ROS	reactive oxygen species
WST-1	2-(4-iodophenyl)-3-(2,4-dinitrophenyl)-5-(2,4-disulfophenyl)-2H-tetrazolium

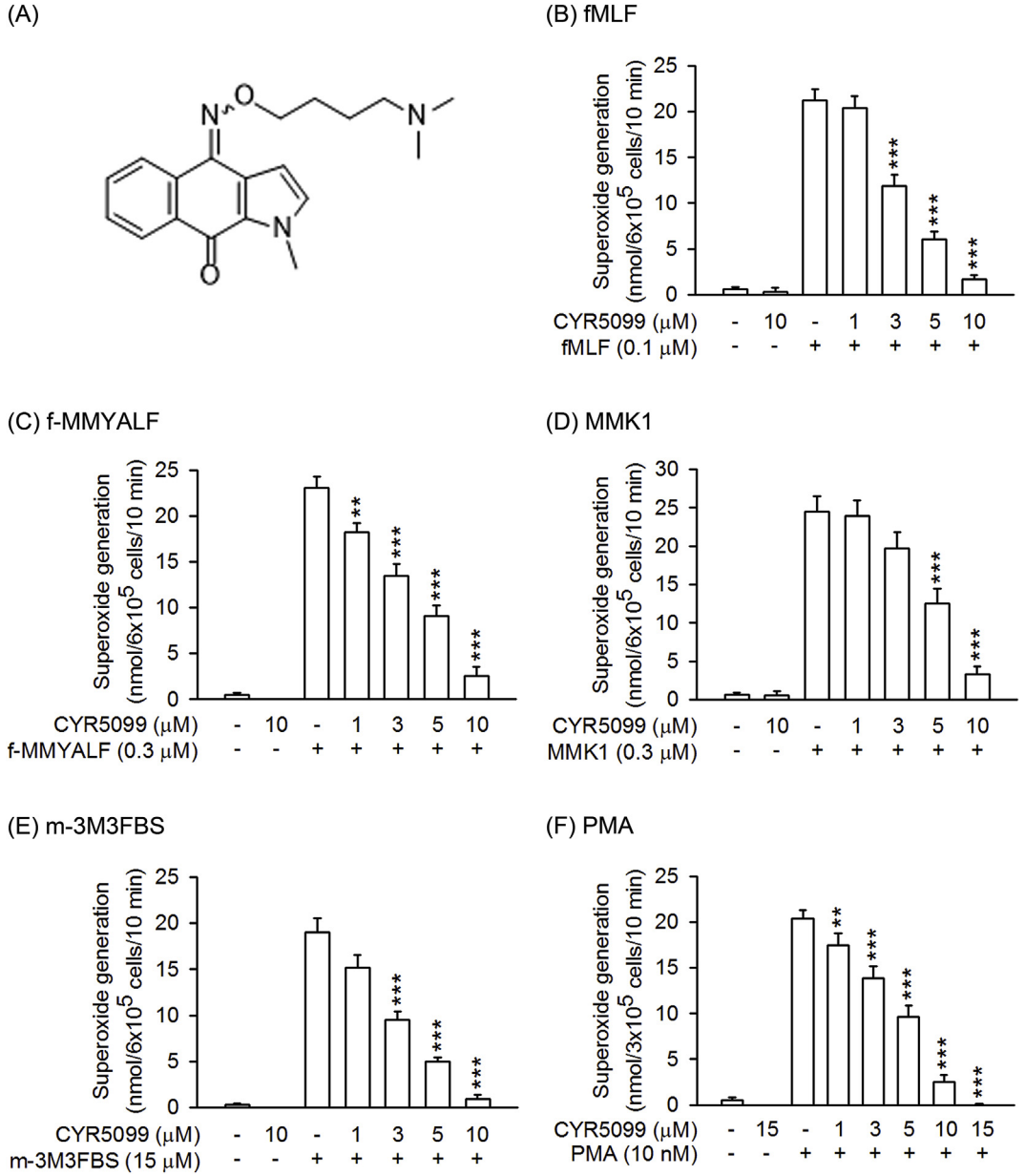

Fig. 1. CYR5099 inhibits superoxide anion generation in activated human neutrophils. (A) The chemical structure of CYR5099. Human neutrophils were incubated with DMSO (0.1%, as control) or CYR5099 (1–10 μM) for 5 min and then activated with (B) fMLF (0.1 μM)/CB (1 μg/ml), (C) f-MMYALF (0.3 μM) and CB (1 μg/ml), (D) MMK1 (0.3 μM)/CB (1 μg/ml), (E) *m*-3M3FBS (15 μM)/CB (1 μg/ml), or (F) PMA (10 nM). Ferricytochrome *c* reduction was monitored by a spectrophotometer at 550 nm. All data are expressed as mean ± S.E.M. (n = 6 or 8). $^{**}p < 0.01$; $^{***}p < 0.001$ compared with activator alone.

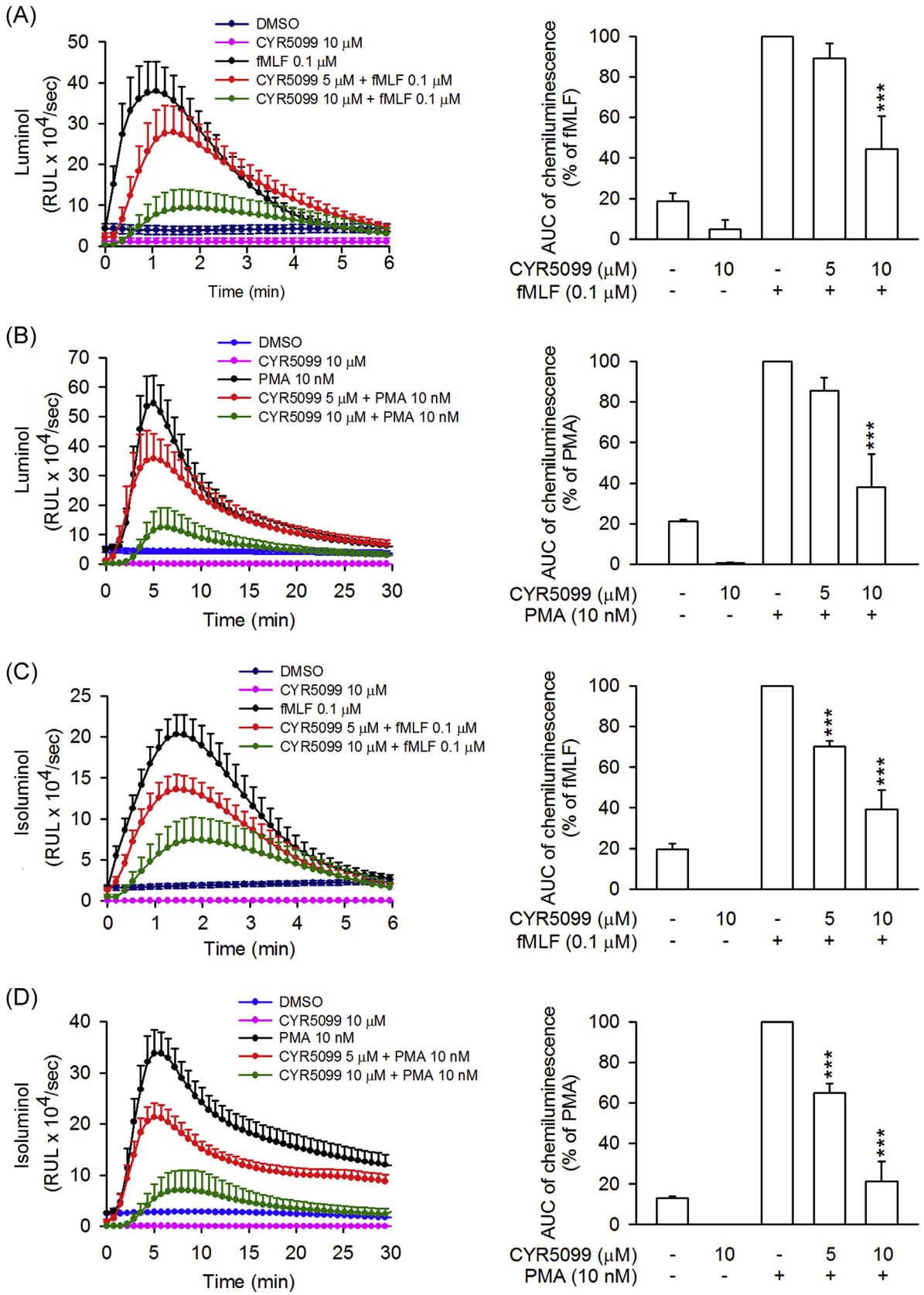

Fig. 2. CYR5099 inhibits total and extracellular ROS generation in activated human neutrophils. Human neutrophils were incubated with DMSO or CYR5099 (5 and 10 μM) for 5 min before stimulation with fMLF (0.1 μM) or PMA (10 nM). (A) Luminol was used to detect total ROS. (B) Isoluminol was used to detect extracellular ROS. Chemiluminescence levels were calculated and data are shown as the mean ± S.E.M. (n = 5). ***$p < 0.001$.

oxidative stress accumulation [10]. Therefore, NOX2 is a promising therapeutic target for treating neutrophil-dominant inflammatory disorders.

Currently, only few drugs are used to inhibit neutrophil dysregulation during inflammation [11–13]. In a search for new anti-inflammatory agents, our laboratory established a platform for randomly screening small molecular compounds in activated human neutrophils. 4-[(4-(Dimethylamino)butoxy)imino]-1-methyl-1H-benzo[f]indol-9(4H)-one (CYR5099) (Fig. 1A), a newly synthesized derivative of benzo[f]indole-4,9-dione, was found to selectively inhibit $O_2^{\bullet-}$ generation but not elastase release in activated human neutrophils. In this study, we identified that CYR5099 acts as a NOX2 inhibitor and effectively inhibits the production of $O_2^{\bullet-}$ and ROS in activated human neutrophils. Therefore, we hypothesized that CYR5099 may have anti-inflammatory effects via inhibiting oxidative stress. Arthritis is a common inflammatory disease characterized by increased ROS and proinflammatory cytokines that cause joint pain, swelling, and stiffness. Excessive ROS generation, particularly via NOX2, contributes to joint inflammation and articular cartilage degradation [3,14]. Complete Freund's adjuvant (CFA) is a known potent inflammatory stimulus used in an experimental arthritis animal model [15–17]. CFA injection has been found to induce an increase of neutrophil infiltration in the arthritis synovium [17,18]. The present study aimed to investigate the effects and molecular action of CYR5099 in human neutrophils and its protective effect in a murine CFA-induced paw inflammation model.

2. Materials and methods

2.1. Reagents

CYR5099 was synthesized by Professors Cherng-Chyi Tzeng and Yeh-Long Chen, Department of Medicinal and Applied Chemistry, Kaohsiung Medical University, Taiwan, and described in Supplementary Fig. 1. Protease inhibitor cocktail tablet was obtained from Roche (Indianapolis, IN, USA). Dulbecco's Modified Eagle Medium (DMEM) and Hank's balanced salts solution (HBSS) were obtained from Gibco (Grand Island, NY, USA). Methoxysuccinyl-Ala-Ala-Pro-Val-*p*-nitroanilide and apocynin was obtained from Calbiochem (La Jolla, CA, USA). Interleukin-8 (IL-8) was obtained from ProSpec (East Brunswick, NJ, USA). 8-Amino-5-chloro-2,3-dihydro-7-phenyl-pyrido[3,4-*d*]pyridazine sodium salt (L-012) and Leu-Glu-Ser-Ile-Phe-Arg-Ser-Leu-Leu-Phe-Arg-Val-Met (MMK-1) were obtained from Tocris Bioscience (Bristol, UK). Leukotriene B4 (LTB4) was purchased from Enzo Life Science (Farmingdale, NY, USA). 2-(4-Iodophenyl)-3-(4-nitrophenyl)-5-(2,4-disulfophenyl)-2H-tetrazolium monosodium salt (WST-1) was obtained from Dojindo (Kunamoto, Japan). Fluo-3 acetomethoxyester (Fluo-3/AM) was obtained from Molecular Probes (Eugene, OR, USA). Anti-rabbit Oregon Green 488, dihydroethidine (HE), Hoechst 33342, and 1,1′-dioctadecyl-3,3,3′,3′-tetramethylindocarbocyanine perchlorate (DiI) were purchased from Invitrogen (Carlsbad, CA, USA). Xanthine were obtained from Santa Cruz Biotechnology (Santa Cruz, CA, USA). The antibodies of p38, phospho-p38 (Thr180/Tyr182), JNK, phospho-JNK (Thr183/Tyr185), Akt (pan), phospho-Akt (Ser473), ERK, phospho-ERK (Thr202/Tyr204), and HRP-linked anti-rabbit IgG were purchased from Cell Signaling (Beverly, MA, USA). Anti-Ly6G antibody was purchased from eBiosciences (San Diego, CA, USA). Anti-myeloperoxidase (MPO) antibody was purchased from (Abcam, Cambridge, MA, USA). Immobilon™ Western chemiluminescence HRP substrate and Millicell® hanging cell culture inserts were obtained from Millipore Sigma (Billerica, MA, USA). Nitrocellulose membrane was obtained from PerkinElmer Inc. (Boston, MA, USA). 2,2′-Azino-bis (3-ethylbenzothiazoline-6-sulfonic acid) (ABTS), cytochalasin B (CB), diphenyleneiodonium (DPI), diphenyl-*p*-picrylhydrazyl (DPPH), ferricytochrome *c*, *N*-formyl-Met-Met-Tyr-Ala-Leu-Phe (f-MMYALF), *N*-formyl-Met-Leu-Phe (fMLF), lipopolysaccharide (LPS), *m*-3M3FBS, phorbol 12-myristate 13-acetate (PMA), platelet activating factor (PAF), zymosan A, α-tocopherol, and xanthine oxidase (XO) were purchased from Sigma-Aldrich (St. Louis, MO, USA).

2.2. Isolation of human neutrophils

This study has been approved by the Institutional Review Board of Chang Gung Memorial Hospital (Registration number: IRB 100 1278C). Informed consent was written and obtained from healthy volunteer. Human neutrophils were isolated according to a standardized procedure: 3% (w/v) dextran sedimentation for 30 min, followed by gradient

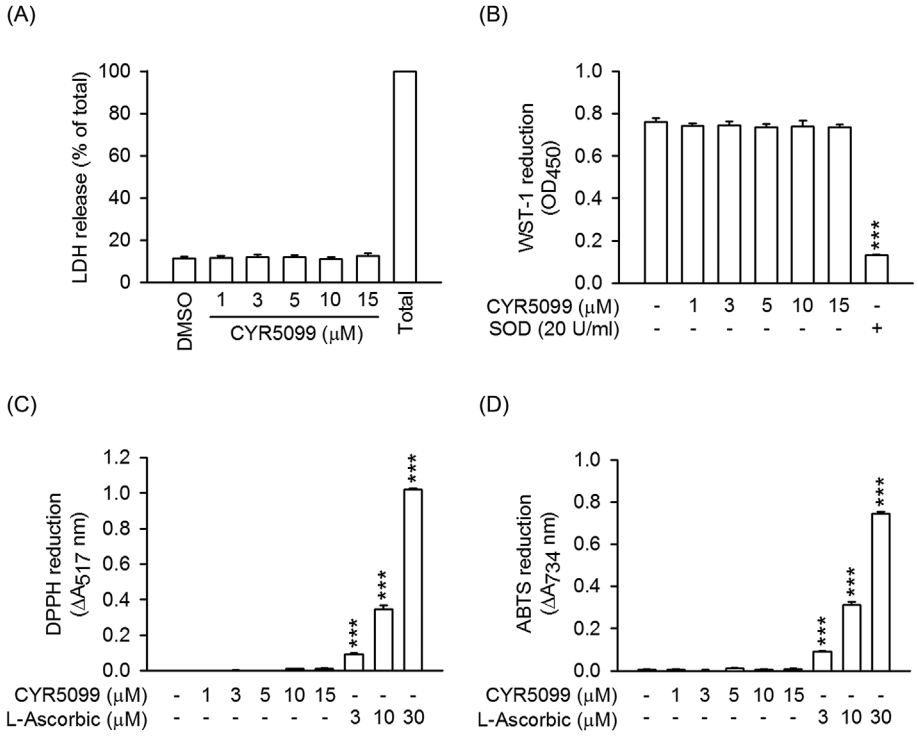

Fig. 3. CYR5099 does not have cytotoxicity and radical-scavenging effects. Human neutrophils were incubated with DMSO or CYR5099 (1–15 μM) for 15 min. (A) LDH release was expressed as percentage of enzyme liberated by incubation with 0.1% Triton X-100. (B) Reduction of WST-1 by xanthine/xanthine oxidase was measured spectrophotometrically at 450 nm. Superoxide dismutase (SOD) was used as positive control. (C) Reduction of DPPH and (D) ABTS was assayed spectrophotometrically at 517 and 734 nm, respectively. L-Ascorbic acid was used as positive control. All data are expressed as the mean ± S.E.M. (n = 3). ***$p < 0.001$ compared with DMSO.

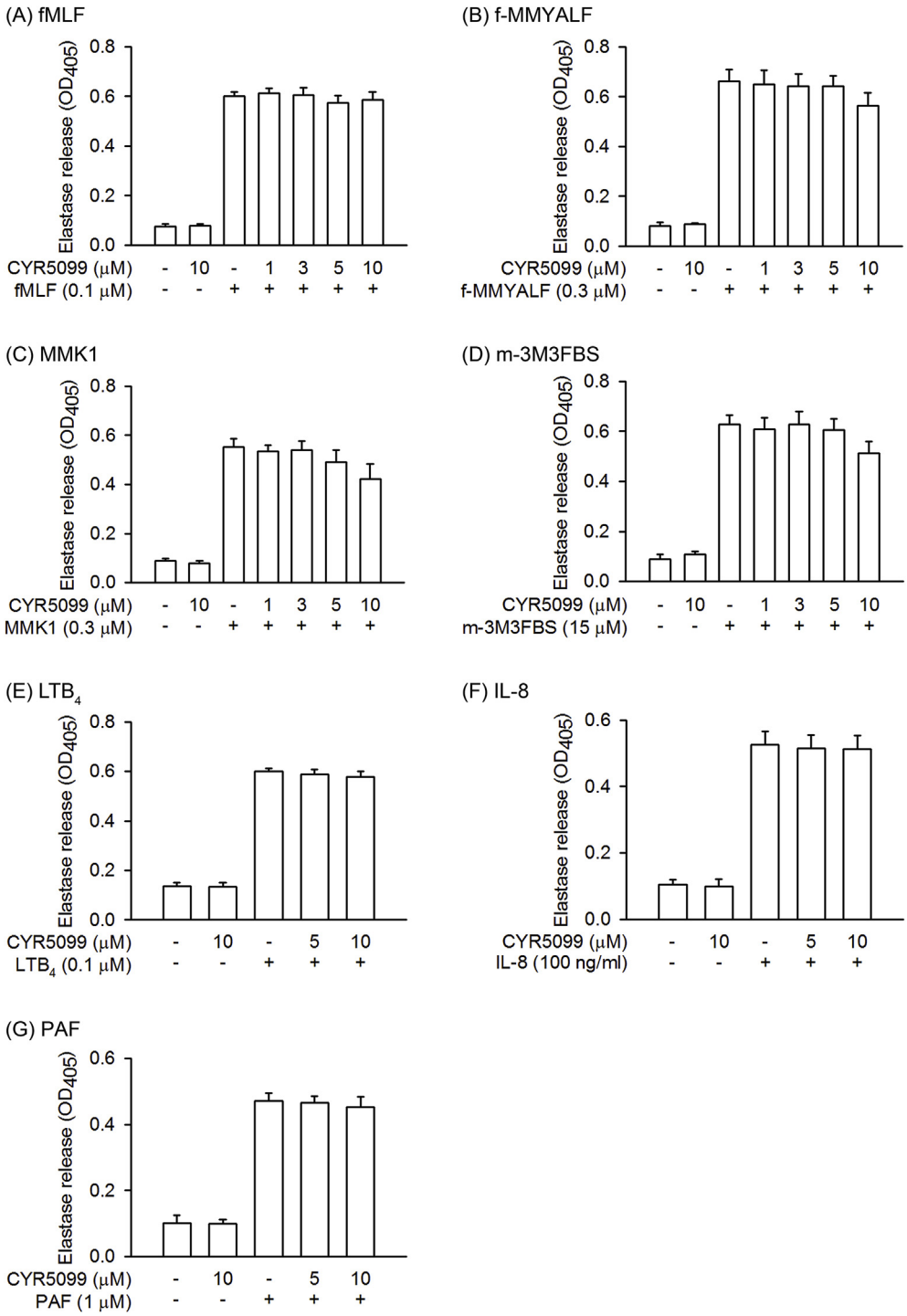

Fig. 4. CYR5099 does not affect elastase release in activated human neutrophils. Human neutrophils were incubated with DMSO or CYR5099 (1–10 μM) for 5 min, and then activated by (A) fMLF (0.1 μM)/CB (0.5 μg/ml), (B) f-MMYALF (0.3 μM)/CB (0.5 μg/ml), (C) MMK1 (0.3 μM)/CB (0.5 μg/ml), (D) *m*-3M3FBS (15 μM)/CB (0.5 μg/ml), (E) LTB_4 (0.1 μM)/CB (0.5 μg/ml), (F) IL-8 (100 ng/ml)/CB (2 μg/ml), or (G) PAF (1 μM)/CB (0.5 μg/ml). Elastase release was measured spectrophotometrically at 450 nm. All data are expressed as mean ± S.E.M. (n = 4 or 6).

centrifugation in Ficoll-Hypaque and hypotonic lysis of erythrocytes. Cell viability of the purified neutrophils was determined using a hemocytometer and the trypan blue-positive neutrophils were determined. Experiments were performed using neutrophils that were > 98% viable. Neutrophils were suspended and maintained in cold HBSS buffer (pH 7.4) without calcium [19].

2.3. Preparation of endothelial cell (ECs)

The murine brain microvascular ECs (bEnd.3) was obtained from the Bioresource Collection Center (Hsinchu, Taiwan). bEnd.3 were cultured in DMEM supplemented with 10% fetal bovine serum (FBS) containing antibiotics in a humidified atmosphere at 37 °C with 5% CO_2. bEnd.3 were passaged every 3 days at 1×10^5 cells/ml after cells reached confluence [20].

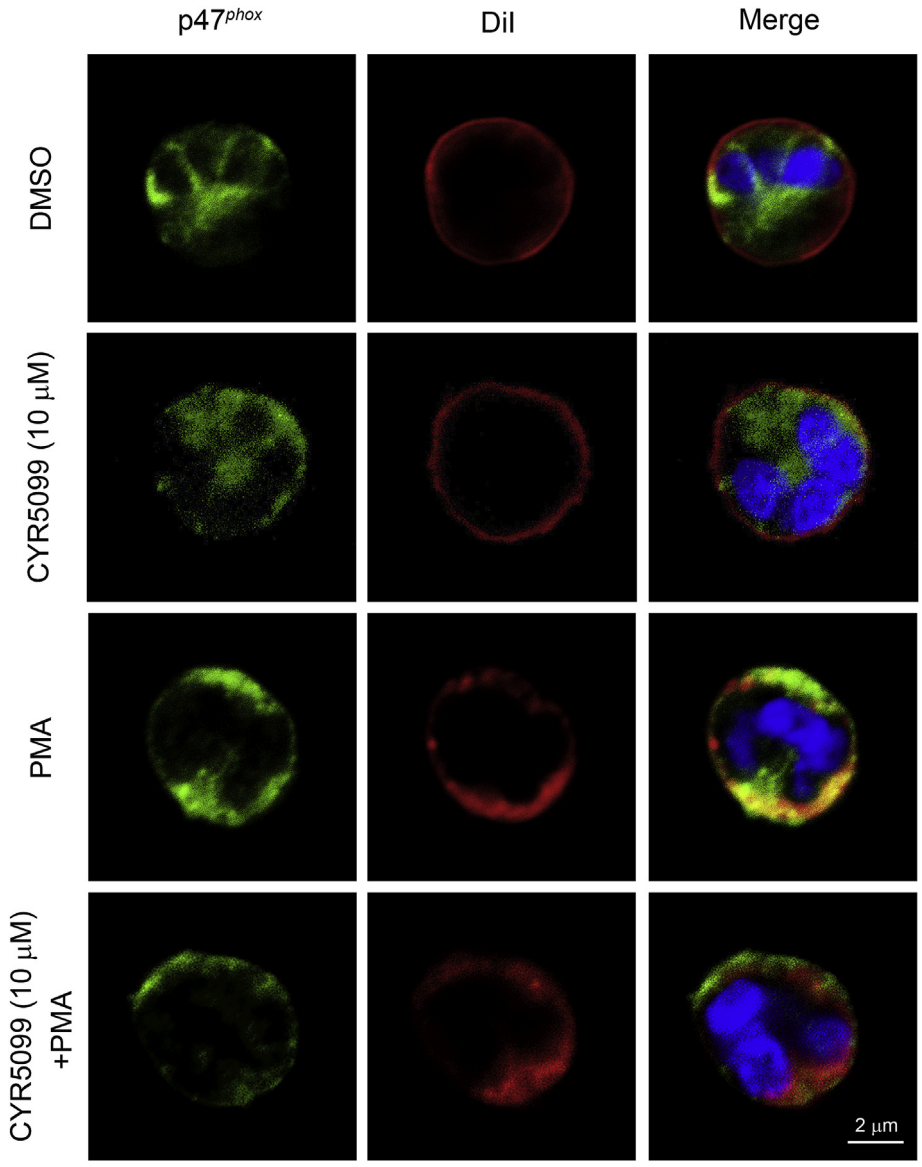

Fig. 5. CYR5099 does not inhibit p47^{phox} translocation in human neutrophils. Human neutrophils were incubated with DMSO or CYR5099 (10 μM) for 5 min, and then activated PMA (10 nM). Cells were fixed with 4% paraformaldehyde and stained with anti-p47^{phox} antibody, DiI, and Hochst 33342. p47^{phox}, DiI, and Hoechst 33342 staining are shown in green, red, and blue, respectively. Co-distribution (orange) was determined by merging the green and red images. Scale bar: 2 μm. (For interpretation of the references to color in this figure legend, the reader is referred to the Web version of this article.)

2.4. Measurement of $O_2^{\bullet -}$ generation

Ferricytochrome *c* was used to measure the amount of $O_2^{\bullet -}$ [21]. Human neutrophils (3×10^5 or 6×10^5 cells/ml) were preincubated with 0.5 mg/ml (40.4 μM) ferricytochrome *c* at 37 °C, and then incubated with DMSO or CYR5099 for 5 min before activation by fMLF (0.1 μM), MMK1 (0.3 μM), f-MMYALF (0.3 μM), *m*-3M3FBS (15 μM) or PMA (10 nM). CB (1 μg/ml) was added to priming neutrophils before stimulators, except for PMA. CB converted neutrophils from phagocytic to secretory cells for facilitating respiratory burst and degranulation via disaggregation of intracellular actin network [22]. The absorbance was monitored continuously using a spectrophotometer at 550 nm.

Luminal or isoluminol enhanced chemiluminescence was used to assay total ROS or extracellular ROS, respectively [19]. Human neutrophils (7×10^5 cells/ml) were preincubated with 37.5 μM luminol or isoluminol in the presence of 6 U/ml horseradish peroxidase at 37 °C, and then incubated with DMSO or CYR5099 for 5 min before activation.

2.5. Analysis of elastase release

Human neutrophils (6×10^5 or 1×10^6 cells/ml) were pre-incubated with methoxysuccinyl-Ala-Ala-Pro-Val-*p*-nitroanilide (elastase substrate, 100 μM) at 37 °C, and then treated with DMSO or CYR5099 for 5 min before activation by fMLF (0.1 μM), f-MMYALF (0.3 μM), MMK1 (0.3 μM), *m*-3M3FBS (15 μM), LTB_4 (0.1 μM), IL-8 (100 ng/ml) or PAF (1 μM) in the presence of CB (0.5 or 2 μg/ml). The absorbance was monitored continuously using a spectrophotometer at 405 nm [23].

2.6. Detection of cytotoxicity

Lactate dehydrogenase (LDH) assay kit (Promega, Madison, WI, USA) was used to determine the cytotoxicity. Human neutrophils were treated with DMSO or CYR5099 for 15 min at 37 °C. Cell-free supernatants were collected and LDH was measured [24].

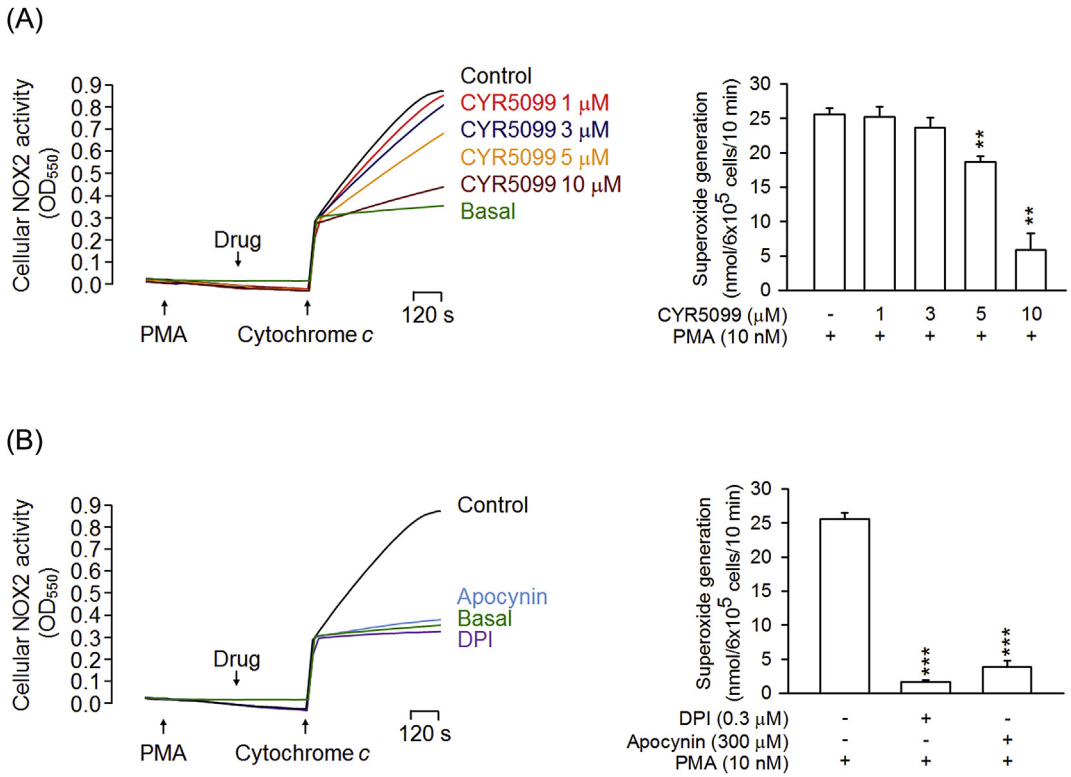

Fig. 6. CYR5099 inhibits NOX2 activity in human neutrophils. Human neutrophils were activated by PMA (10 nM) for 5 min, and then incubated with (A) CYR5099 (5099, 1–10 μM) or (B) DPI (0.3 μM) and apocynin (300 μM) for another 5 min. NOX2-mediated superoxide anion generation was measured by adding ferricytochrome c (0.5 mg/ml). All data are expressed as mean ± S.E.M. (n = 3) from. $^{**}p < 0.01$; $^{***}p < 0.001$ compared with PMA alone.

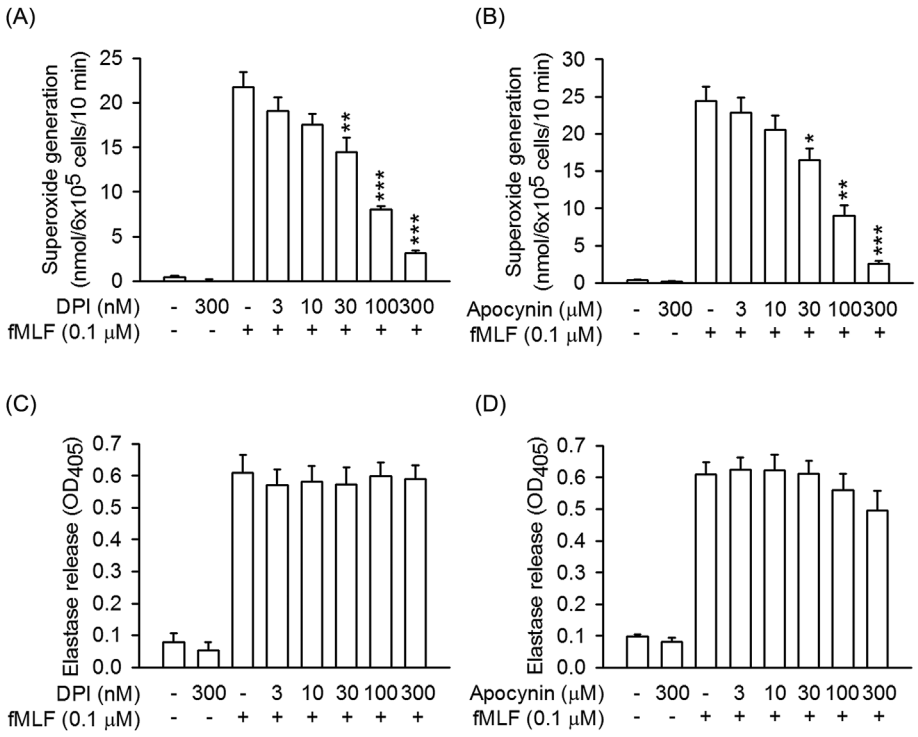

Fig. 7. DPI and apocynin inhibit superoxide anion generation, but not elastase release, in activated human neutrophils. Human neutrophils were incubated with DMSO, (A and C) DPI (3–300 nM), or (B and D) apocynin (3–300 μM) for 5 min, and then activated by fMLF/CB for another 10 min. (A and B) Superoxide anion and (C and D) elastase release were measured. All data are expressed as mean ± S.E.M. (n = 5). $^{*}p < 0.05$; $^{**}p < 0.01$; $^{***}p < 0.001$ compared with fMLF alone.

2.7. $O_2^{\bullet -}$ and free radical scavenging assay

The scavenging effects of CYR5099 on $O_2^{\bullet -}$ or free radicals were determined in cell-free xanthine/xanthine oxidase (XO), DPPH, or ABTS assays [25].

2.8. NOX2 activity assay

Cellular NOX2 activity was measured in human neutrophils. Neutrophils (6×10^5 cells/ml) were preincubated with PMA (10 nM) at 37 °C for 5 min, and treated with DMSO, CYR5099 or NOX2 inhibitors

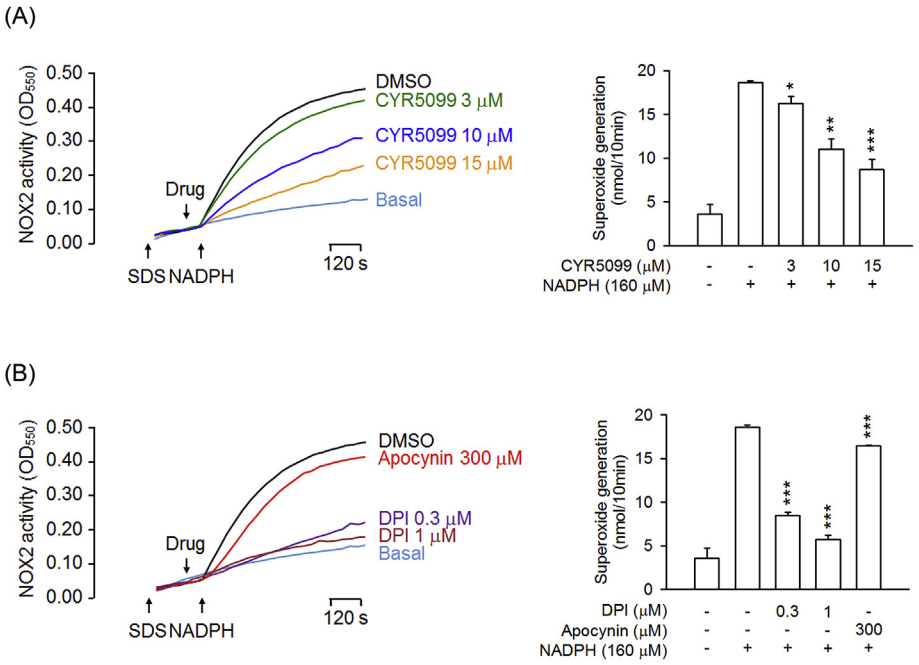

Fig. 8. CYR5099 inhibits NOX2 activity. A mixture of cytosolic and membrane fractions from neutrophils was pretreated with SDS (100 μM) for 2 min, and then incubated with (A) CYR5099 (3, 10, and 15 μM) or (B) DPI (0.3 and 1 μM) and apocynin (300 μM). The reaction was initiated by adding NADPH (160 μM). All data are expressed as mean ± S.E.M. (n = 3). *$p < 0.05$; **$p < 0.01$; ***$p < 0.001$ compared with control.

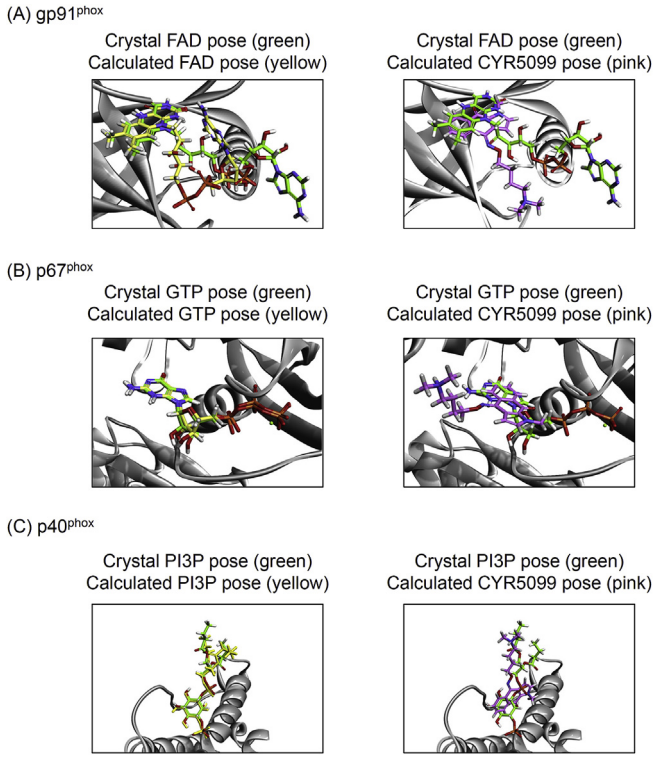

Fig. 9. CYR5099 is proposed to selectively bind to gp91^{phox} *in vitro*. The crystal *in-situ* structures of (A) FAD-targeted gp91^{phox}, (B) GTP-targeted p67^{phox}, and (C) PI3P-targeted p40^{phox} were adopted from PDB 5O0X, 1E96, and 1H6H, respectively (crystal pose; green color). The calculated *in-situ* structures of (A) FAD- and CYR5099-targeted gp91^{phox}, (B) GTP- and CYR5099-targeted p67^{phox}, and (C) PI3P- and CYR5099-targeted p40^{phox} (calculated pose; yellow and pink color, respectively). (For interpretation of the references to color in this figure legend, the reader is referred to the Web version of this article.)

(apocynin and DPI) for 5 min. $O_2^{\bullet -}$ generation by NOX2 was assayed by the addition of ferricytochrome *c* (0.5 mg/ml).

Subcellular NOX2 activity was also determined. Neutrophils were preincubated with protease inhibitor cocktail tablet (1/1000; Roche, Indianapolis, IN, USA) for 30 min at 4 °C, and then cells were sonicated in NOX2 assay buffer (pH 7.3; 100 mM KCl, 10 mM PIPES, 3 mM NaCl, 1 mM EGTA, 3.5 mM $MgCl_2$, and 1 mM ATP). Nonruptured neutrophils were removed by centrifugation at 300 × *g* for 5 min. The cytosolic and membrane fractions were isolated by centrifugation at 14,000 × *g* for 30 min at 4 °C. The cytosol fraction and membrane fraction were mixed in reaction buffer (10 mM $NaH_2PO_4/Na_2HPO_4.12H_2O$, 2.7 mM KCl, 138 mM NaCl, 2 mM $MgCl_2$, 2 μM GTPγS, and 0.5 mg/ml ferricytochrome *c*; pH 7.4) at 30 °C. NOX2 was activated with the addition of 100 μM sodium dodecyl sulfate (SDS) before the addition of DMSO, CYR5099, apocynin, or DPI. The absorbance was monitored continuously using a spectrophotometer at 550 nm [21].

2.9. Measurement of intracellular calcium concentration ($[Ca^{2+}]_i$)

Human neutrophils (3 × 10^6 cells/ml) were labeled with fluo-3/AM (2 μM) at 37 °C for 35 min. Labeled neutrophils were preincubated with DMSO or CYR5099 for 5 min, and then activated by fMLF (0.1 μM), f-MMYALF (0.3 μM), MMK1 (0.3 μM), *m*-3M3FBS (15 μM), LTB_4 (0.1 μM), IL-8 (100 ng/ml), or PAF (1 μM). The changes of fluorescence were monitored continuously using a spectrofluorometer [26].

2.10. Immunoblotting analysis

Neutrophils were treated with DMSO or CYR5099 for 5 min, and then activated with fMLF (0.1 μM)/CB (0.5 μg/ml) for 25 s. The reaction was stopped by the addition of sample buffer (62.5 mM pH 6.8 Tris-HCl, 4% sodium dodecyl sulfate (SDS), 5% β-mercaptoethanol, 0.0125% bromophenol blue, and 8.75% glycerol) at 100 °C for 15 min. Whole-cell lysates were obtained by centrifugation at 14,000 × *g* for 20 min at 4 °C. Phosphorylation of MAPKs and Akt was assayed by immunoblotting with the corresponding rabbit antibodies (1:2000) and HRP-linked anti-rabbit IgG antibodies (1:10000). The phosphorylated and total proteins were identified using enhanced chemiluminescence kits, and evaluated using a densitometer (UVP, Upland, CA, USA) [27].

2.11. Analysis of CD11b expression

Human neutrophils were pretreated with DMSO or CYR5099 for

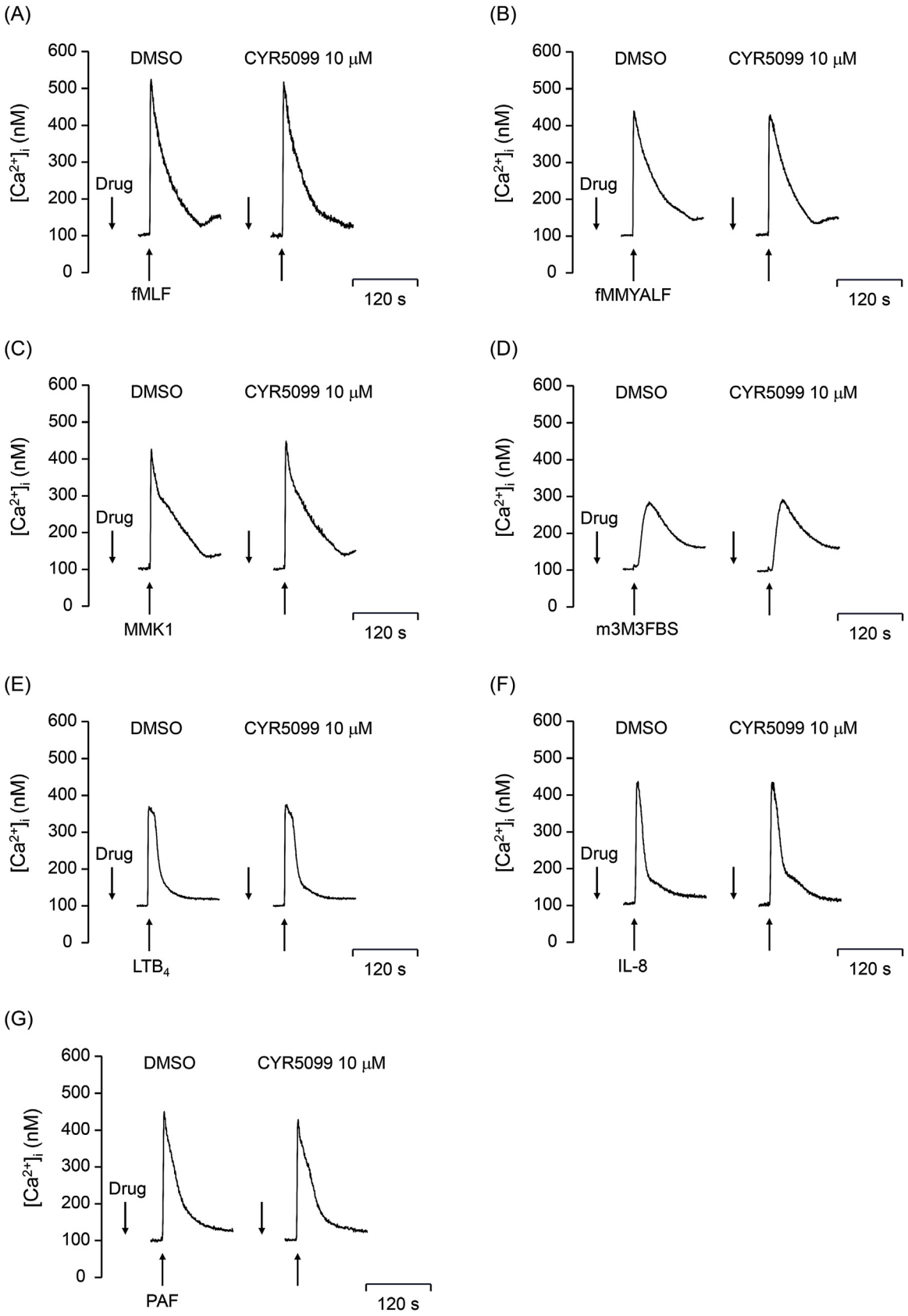

Fig. 10. CYR5099 does not alter Ca^{2+} mobilization in activated human neutrophils. Fluo-3-labeled human neutrophils were incubated with DMSO or CYR5099 (10 μM) for 5 min, and then activated by DMSO, (A) fMLF (0.1 μM), (B) f-MMYALF (0.3 μM), (C) MMK1 (0.3 μM), (D) *m*-3M3FBS (15 μM), (E) LTB_4 (0.1 μM), (F) IL-8 (100 ng/ml), or (G) PAF (1 μM). Ca^{2+} mobilization was determined in real-time using a spectrofluorometer. Representative traces of Ca^{2+} mobilization are shown (n = 3 or 4).

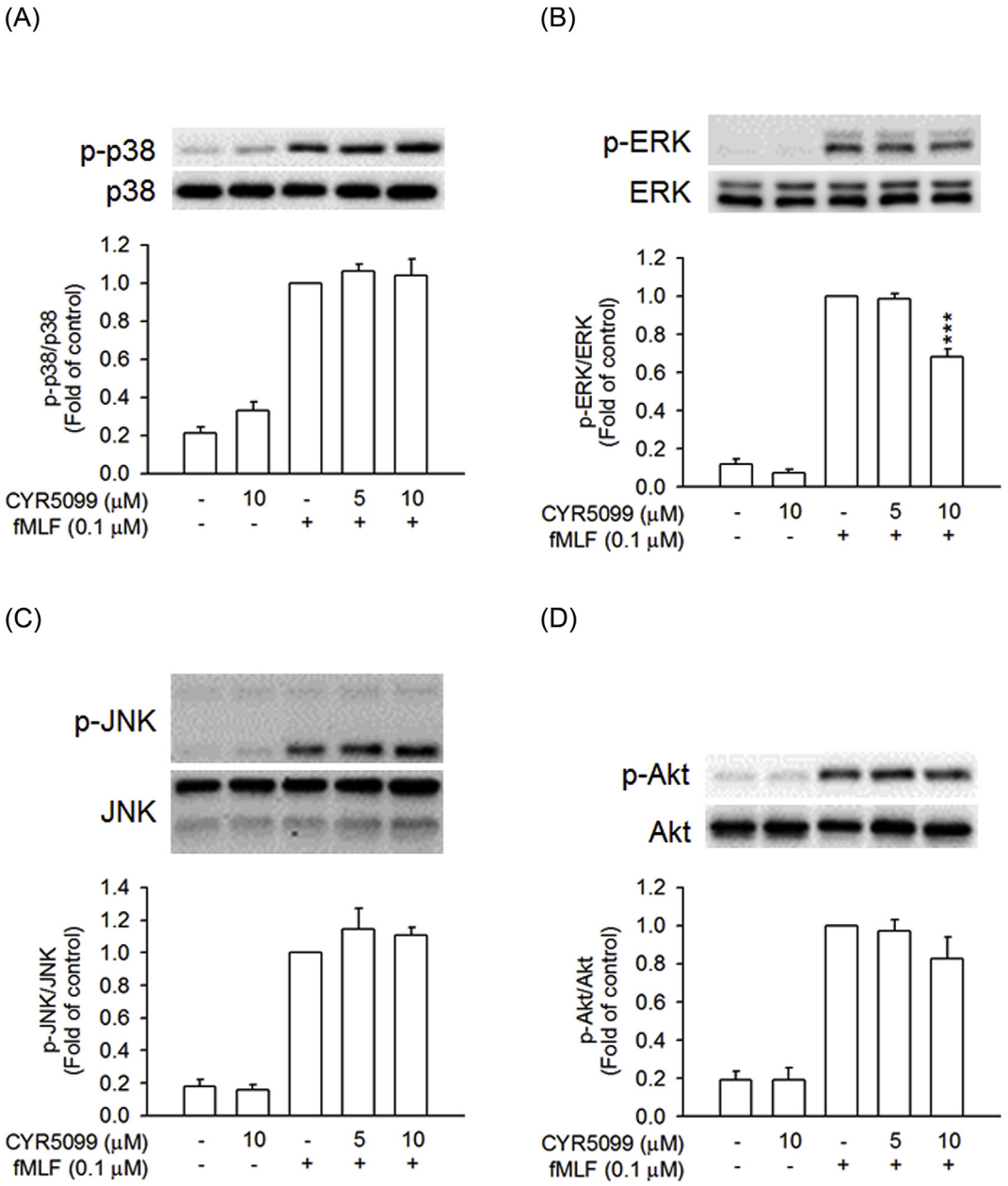

Fig. 11. Effects of CYR5099 on phosphorylation of MAPKs and Akt in fMLF-activated human neutrophils. Human neutrophils were incubated with DMSO or CYR5099 (5 and 10 μM) for 5 min, and then activated by fMLF (0.1 μM)/CB (0.5 μg/ml) for 25 s. Phosphorylation of (A) p38, (B) ERK, (C) JNK, or (D) Akt was assayed by Western blot. All data are expressed as mean ± S.E.M. (n = 3–4). ***$p < 0.001$ compared with fMLF alone.

5 min and then activated by fMLF (0.1 μM)/CB (0.5 μg/ml) or PMA (10 nM) for another 5 min. After centrifugation at 200 × *g* for 8 min at 4 °C, cells were re-suspended in HBSS with 0.5% BSA and FITC-labeled anti-CD11b mouse monoclonal antibody (12.5 μg/ml) for 90 min CD11b expression was examined by flow cytometry [25].

2.12. Neutrophil adhesion detection

Human neutrophils were pre-incubated with Hoechst 33342 for 10 min and then centrifuged at 200 × *g* for 8 min to discard the supernatant. Hoechst 33342-labeled human neutrophils were treated with DMSO or CYR5099 for 5 min and then activated by fMLF (0.1 μM)/CB (0.5 μg/ml) for 10 min. Afterwards, cells were co-cultured with LPS (2 μg/ml)-pretreated bEnd.3 cells for 15 min. Non-adherent neutrophils were removed by gentle washing with HBSS and neutrophils adhered to bEnd.3 were counted in 6 fields by microscopy [20,28].

2.13. Immunofluorescence staining

Human neutrophils were incubated on fibrinogen (1 mg/ml)-coated glass slides at 37 °C for 30 min, and then treated with DMSO or CYR5099 for 5 min before activating by PMA (10 nM) for an additional 5 min. Cells were fixed with 4% paraformaldehyde, washed three times with PBS, and permeabilized with 0.05% (w/v) Triton X-100. Afterwards, cells were soaked three times with 0.15 M glycine/PBS, and blocked with 5% goat serum for 1 h at 4 °C. Cells were incubated with anti-$p47^{phox}$ antibody (1:500) overnight at 4 °C, followed by incubation with secondary Oregon Green 488-conjugated anti-rabbit IgG antibody (1:1000) for 1 h. Cells were then washed with 0.15 M glycine/PBS and stained with Hoechst 33342 (1 ng/ml) and DiI (1 ng/ml) for 10 min at room temperature. Images were collected by Zeiss LSM 510 Meta confocal microscopy [24].

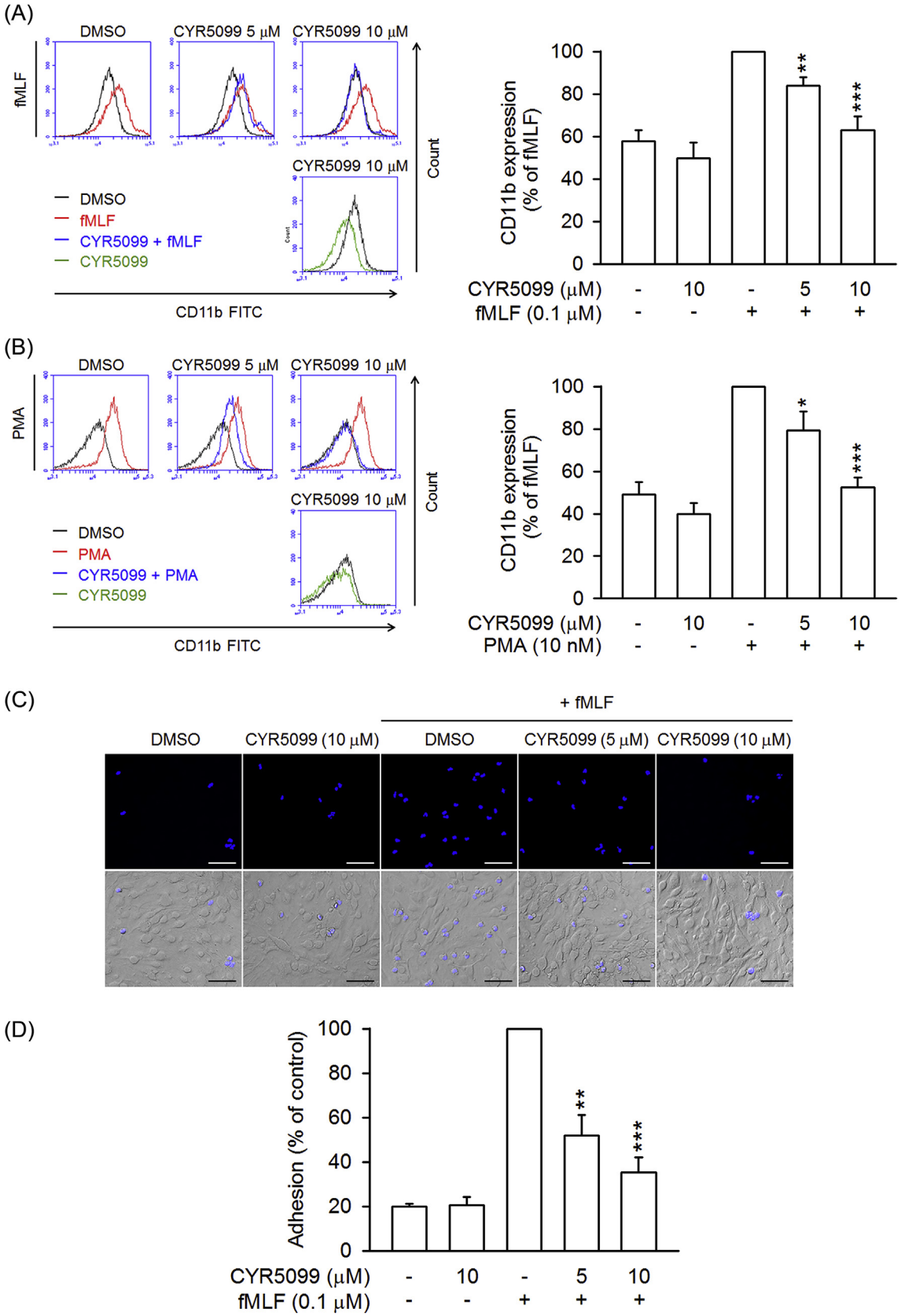

Fig. 12. CYR5099 inhibits human neutrophil CD11b expression and adhesion. Human neutrophils were incubated with DMSO or CYR5099 (5 and 10 μM) for 5 min, and then activated by (A) fMLF (0.1 μM)/CB (0.5 μg/ml) or (B) PMA (10 nM) for an additional 5 min. The fluorescent intensity was determined by FACS using FITC-labeled anti-CD11b antibody. Fluorescence intensities of CD11b are represented as mean ± S.E.M. (n = 6). (C) Hoechst 33342-labelled human neutrophils were incubated with DMSO or CYR5099 (5 and 10 μM), and activated by fMLF (0.1 μM)/CB (0.5 μg/ml). Drug-treated neutrophils were then co-incubated for 15 min with LPS-preincubated bEnd.3. Adherent neutrophils were detected by fluorescent microscopy. Bar = 100 μm. Representative images are shown. (D) Data from (C) are expressed as mean ± S.E.M. (n = 3). $^{*}p < 0.05$; $^{**}p < 0.01$; $^{***}p < 0.001$ compared with fMLF or PMA alone.

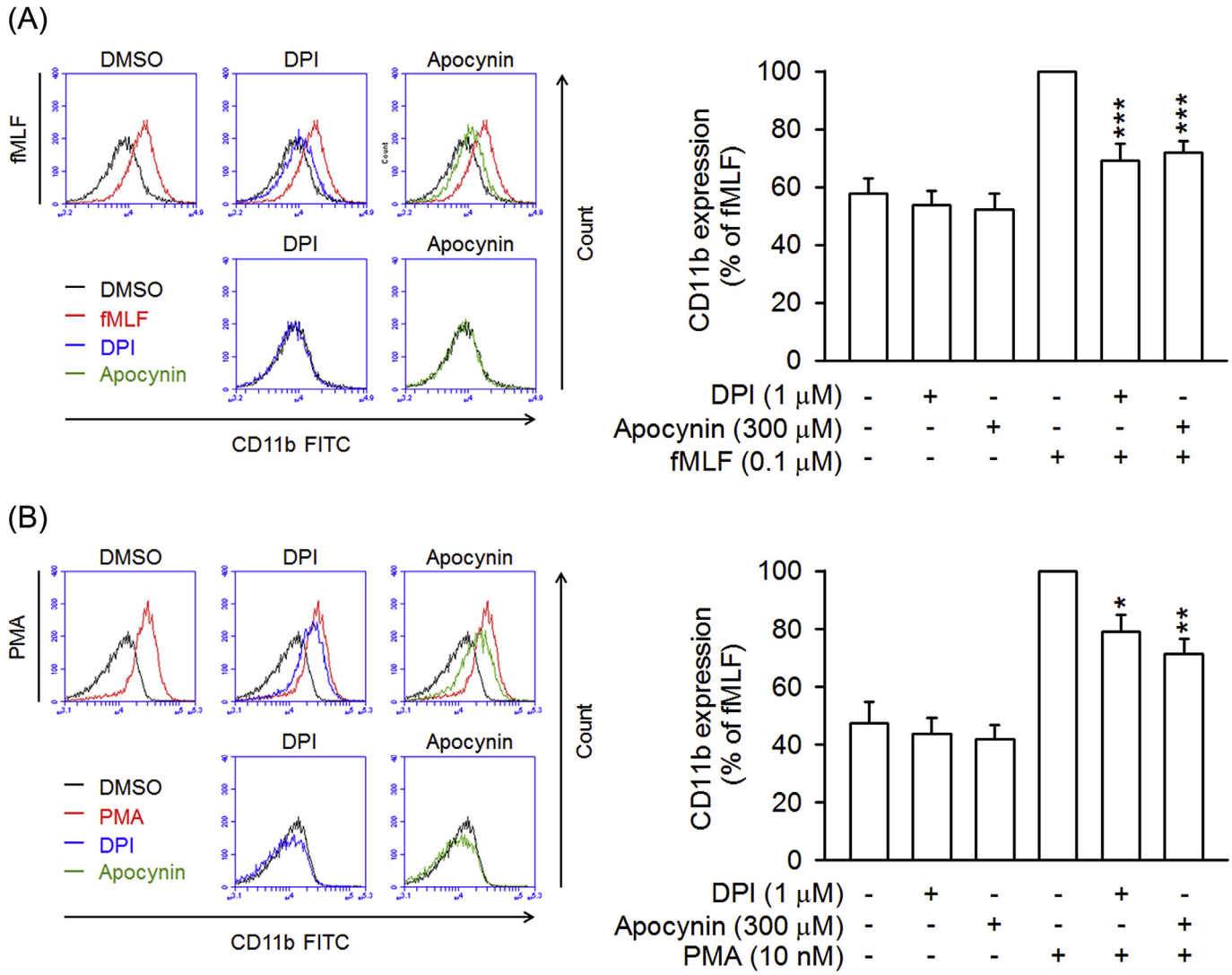

Fig. 13. DPI and apocynin inhibits CD11b expression in activated human neutrophils. Human neutrophils were incubated with DMSO, DPI (1 μM), or apocynin (300 μM) for 5 min, and then activated by (A) fMLF (0.1 μM)/CB (0.5 μg/ml) or (B) PMA (10 nM) for an additional 5 min. The fluorescent intensity was determined by FACS using FITC-labeled anti-CD11b antibody. Fluorescence intensities of CD11b are represented as mean ± S.E.M. (n = 4 or 5). *$p < 0.05$; **$p < 0.01$; ***$p < 0.001$ compared with fMLF or PMA alone.

2.14. Protein preparation and molecular docking

The crystal structure of $p67^{phox}$ and $p40^{phox}$ were obtained from the Protein Data Bank (PDB; accession code: 1E96 and 1H6H, respectively). The remodeling structure of human $gp91^{phox}$ was superimposed from the C-terminal human gp91phox (PDB 3A1F) and FAD-binding region of *C. stagnale* NADPH oxidase (PDB 5O0X) using MODELLER (Supplementary Fig. 2). All structures were prepared to fix commonly problems and protonated at pH 7.4. The 2D structure of CYR5099 was sketched by BIOVIA draw and transfer to 3D coordinates using Catalyst.

CYR5099 was docked to $gp91^{phox}$, $p67^{phox}$, or $p40^{phox}$ protein using CDOCKER program (Dassault Systèmes BIOVIA, Discovery Studio Modeling Environment, Release 2019, San Diego: Dassault Systèmes, 2019). The conformational differences between crystal and calculated substrates were evaluated by RMSD value for each NOX2 subunit. CDOCKER interaction energy and binding energy (ΔG_{bind}) were employed to prioritize the potential target of CYR5099.

2.15. Complete Freund's adjuvant (CFA)-induced paw inflammation

C57BL/6 male mice (7–8 weeks) were housed in an air-conditioned room with 12 h light–dark cycle, and animal studies were conducted according to the guidelines and protocol approved by Institutional Animal Care and Use Committee at Chang Gung University, Taiwan (IACUC approval No. CGU14-150). Mice were injected subcutaneously with carprofen (5 mg/kg) as analgesia and then intraperitoneally with CYR5099 (10 or 25 mg/kg body weight) or an equal volume of 0.9% saline under anesthesia (Isoflurane). After 1 h, paw inflammation was induced by intraplantar injection of CFA (1.5 mg/kg body weight in right-rear foot) or 0.9% saline (left-rear foot; as control). The change in paw thickness (nm) was determined before (baseline) and after CFA/saline injection at the indicated times. After injection of CFA for 4 h, L-012 (25 mg/kg body weight) was intraperitoneally administered. ROS production was determined using a Xenogen IVIS100 imaging system (PerkinElmer, Waltham, MA, USA) under anesthesia (30 mg/kg Zoletil 50 and 6 mg/kg xylazine) [17,29]. CO_2 euthanasia was used to stop the experiments. The hind paws were removed, fixed using 10% neutral buffered formalin, and embedded in paraffin blocks before cutting into 5-μm-thick sections. The staining of hematoxylin and eosin (H&E) and immunohistochemistry (Ly6G and MPO) was performed as previously described [17].

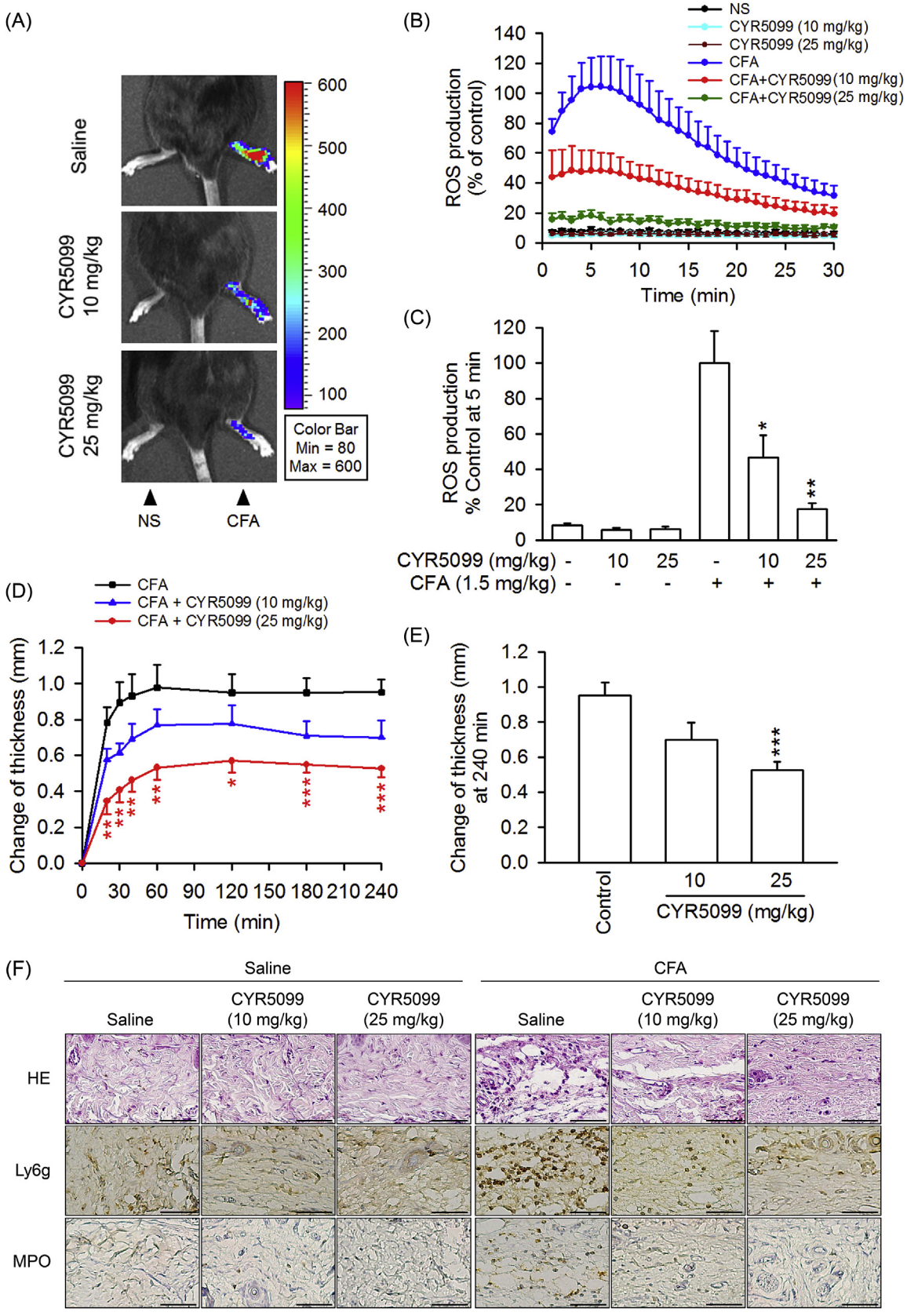

Fig. 14. CYR5099 ameliorates Freund's adjuvant (CFA)-induced paw injury in C57BL/6 mice. Mice were injected with CYR5099 (10 and 25 mg/kg body weight, intraperitoneally) or an equal volume of 0.9% saline for 1 h before injecting CFA (1.5 mg/kg body weight) into the intraplantar space in the hind paw. After CFA injection for 4 h, animals were administered L-012 (25 mg/kg body weight, intraperitoneally). (A) Representative chemiluminescent photos of paw edema are shown using a Xenogen IVIS 100 imaging system. (B) ROS generation from (A). (C) Peak ROS production was shown at 5 min after L-012 injection. (D) Paw thickness was measured with a digital Vernier caliper at the indicated times after CFA injection. (E) Paw edema was determined at 240 min after induction. (F) Representative staining photos of H&E, Ly6G, and MPO are shown. Bar = 50 μm. All data are expressed as the mean ± S.E.M (n = 6). *$p < 0.5$; **$p < 0.01$ compared with the CFA alone.

2.16. Statistical analysis

Statistical analyses were performed with SigmaPlot 8.02 (Systat Software, San Jose, CA, USA) and significance was calculated using Student's *t*-test. All data were normally distributed and expressed as the mean ± standard error of the mean (S.E.M.). A value of $p < 0.05$ was considered statistically significant.

3. Results

3.1. CYR5099 significantly decreases $O_2^{\bullet-}$ and ROS production, but not elastase release, in activated human neutrophils

To examine the anti-inflammatory effects of CYR5099 in human neutrophils, the $O_2^{\bullet-}$ generation and ROS production were analyzed. CYR5099 does-dependently (1–15 μM) inhibited $O_2^{\bullet-}$ generation in human neutrophils activated by fMLF (bacterial formyl peptide receptor (FPR)1 activator), f-MMYALF (mitochondrial FPR1 activator), MMK1 (FPR2 activator), *m*-3M3FBS (phospholipase C activator) and PMA (protein kinase C activator) (Fig. 1). The IC_{50} values of CYR5099 are 3.27 ± 0.03 μM for fMLF, 3.77 ± 0.79 μM for f-MMYALF, 5.19 ± 0.49 μM for MMK1, 2.80 ± 0.27 μM for *m*-3M3FBS, and 4.74 ± 0.51 μM for PMA. Using the specific 2-hydroxyethidium quantification assay to detect $O_2^{\bullet-}$, CYR5099 (1, 3, and 10 μM) significantly inhibited the $O_2^{\bullet-}$ generation in fMLF-activated human neutrophils (Supplementary Fig. 3). In addition, luminal and isoluminol-enhanced chemiluminescence assays indicated that CYR5099 significantly decreased total and extracellular ROS generation induced by fMLF and PMA (Fig. 2). CYR5099 also restricted total ROS production in human neutrophils stimulated by zymosan A, a pathogen prepared from *S. cerevisiae* (Supplementary Fig. 4). These results indicated that CYR5099 has anti-inflammatory effects through inhibiting human neutrophil oxidative stress. CYR5099 did not induce LDH release in human neutrophils, even in the presence of activators (fMLF or PMA), and it did not have $O_2^{\bullet-}$ and free radicals-scavenging activity in cell-free xanthine/xanthine oxidase, DPPH, or ABTS assays (Fig. 3 **and** Supplementary Fig. 5), ruling out the anti-inflammatory effects were due to cytotoxicity or direct $O_2^{\bullet-}$-scavenging.

Elastase release is an important indicator of neutrophil degranulation. To determine whether CYR5099 has inhibitory effect on degranulation, elastase release was monitored. CYR5099 did not affect elastase release in human neutrophils activated by fMLF, f-MMYALF, MMK1, *m*-3M3FBS, LTB_4, IL-8, and PAF (Fig. 4).

3.2. CYR5099 inhibits NOX2 activity

NOX2 activation is dependent on phosphorylation of $p47^{phox}$, a cytosolic component of the enzyme. $p47^{phox}$ phosphorylation stimulates translocation of the cytosolic components to the membranes to induce NOX2 activation [30,31]. Our result indicated that CYR5099 failed to alter PMA-induced $p47^{phox}$ phosphorylation and translocation to membrane in human neutrophils (Fig. 5 **and** Supplementary Fig. 6), ruling out that the inhibition of $O_2^{\bullet-}$ and ROS production by CYR5099 was through regulating NOX2 upstream pathways.

To further examine the inhibitory effect of CYR5099 on NOX2, cellular and subcellular NOX2 activities were measured. In the cellular system, CYR5099 inhibited NOX2-mediated $O_2^{\bullet-}$ generation in PMA-preactivated human neutrophils (Fig. 6A). DPI and apocynin are two well-studied inhibitor of NOX2 [32]. In this study, DPI (0.3 μM) and apocynin (300 μM) were used as positive controls and showed significant inhibition (Fig. 6B). Furthermore, DPI (3–300 nM) and apocynin (3–300 μM) inhibited $O_2^{\bullet-}$ production, but not elastase release, in fMLF-activated human neutrophils (Fig. 7).

We suggest that CYR5099 may act as an inhibitor of NOX2. To identify this hypothesis, NOX2 activity assay was performed in subcellular experiments. Noticeably, our data showed that CYR5099 and DPI reduced the NOX2 activity in SDS-reconstituted subcellular assay (Fig. 8). Therefore, CYR5099 is a new NOX2 inhibitor and can inhibit respiratory burst in human neutrophils. Interestingly, apocynin did not significantly inhibit subcellular NOX2 activity. A possible explanation is that apocynin is a prodrug. Apocynin requires MPO and H_2O_2 to form an activate apocynin radical and dimer [33–36].

NOX2 is comprised of $gp91^{phox}$ (NOX2), $p22^{phox}$, $p47^{phox}$, $p67^{phox}$, $p40^{phox}$, and Rac2 in neutrophils [5,6]. The molecular docking of CYR5099 with NOX2 subunits was performed to determine how CYR5099 blocked the NOX2 activity. CDOCKER interaction energy and CHARMm forcefield were employed for the molecular dynamics scheme to dock ligands into a protein binding site. The crystal *in-situ* structures of FAD-targeted $gp91^{phox}$, GTP-targeted $p67^{phox}$, and phosphatidylinositol 3-phosphate (PI3P)-targeted $p40^{phox}$ were remodeled and modified from PDB 5O0X, 1E96, and 1H6H, respectively. The RMSD values between the crystal and calculated *in-situ* structures were estimated as 5.87 Å, 0.60 Å, and 1.96 Å, respectively. The CDOCKER energy values of calculated *in-situ* structures were 41.94, 169.50, and 131.31 −kcal/mol, respectively. Importantly, the CDOCKER energy values of CYR5099-targeted $gp91^{phox}$, CYR5099-targeted $p67^{phox}$, and CYR5099-targeted $p40^{phox}$ were 38.62, 27.38, and 10.21 −kcal/mol, respectively (Fig. 9). Based on molecular docking results, we suggest that CYR5099 may selectively target $gp91^{phox}$, a specific subunit of NOX2.

To further examine the selectivity of CYR5099, we detected the ROS generation in HT-29 cells, which highly expressed NOX1 but not other NOX types [37,38]. DPI (0.3 and 3 μM) and apocynin (10 and 30 μM) but not CYR5099 (5 and 10 μM) apparently inhibited NOX1-dependent ROS generation (Supplementary Fig. 7). Using neutrophil-like differentiated HL-60 (dHL-60) cells [39], both CYR5099 (5 and 10 μM) and $p47^{phox}$ knockdown clearly inhibited the PMA-induced superoxide anion generation. Additionally, CYR5099 (5 and 10 μM) failed to further repress the superoxide anion generation in $p47^{phox}$-knockdown dHL-60 cells (Supplementary Fig. 8), suggesting that CYR5099 may be a selective inhibitor of NOX2.

3.3. CYR5099 does not significantly alter Ca^{2+} mobilization and activity of MAPKs and Akt in human neutrophils

Ca^{2+} signals play a key role in several neutrophil functions. To access whether CYR5099 influences Ca^{2+} signaling in activated human neutrophils, intracellular Ca^{2+} concentration ($[Ca^{2+}]_i$) was measured. Our results showed that CYR5099 did not affect $[Ca^{2+}]_i$ in human neutrophils activated by fMLF, f-MMYALF, MMK1, *m*-3M3FBS, LTB_4, IL-8, or PAF (1 μM) (Fig. 10).

Additionally, MAPKs and Akt play important roles in neutrophil inflammatory responses [17,19]. Treatment with fMLF caused rapid activation of p38 MAPK, ERK, JNK, and Akt in human neutrophils. CYR5099 did not affect the phosphorylation of p38 MAPK, JNK, and Akt. However, CYR5099 at high concentration of 10 μM had a minor inhibitory effect on ERK phosphorylation (Fig. 11).

3.4. CYR5099 inhibits neutrophil CD11b expression and adhesion to ECs

CD11b/CD18 is an important integrin for neutrophil adhesion to endothelium [40]. Treatment with fMLF and PMA induced increases in CD11b expression in human neutrophils. CYR5099 significantly reduced fMLF and PMA-induced CD11b expression (Fig. 12A and B). Likewise, fMLF-induced human neutrophil adhesion to bEnd.3 was inhibited by CYR5099 (Fig. 12C and D). Both DPI and apocynin also showed significant inhibitory effects on CD11b expression (Fig. 13), suggesting that NOX2-mediated ROS may involve in integrin expression.

3.5. CYR5099 ameliorates CFA-induced arthritis inflammation

The *in vivo* effect of CYR5099 was investigated in CFA-induced

arthritis inflammation in mice. CFA treatment caused an increase in ROS generation and edema in mouse paw. The histology of paw sections showed that CFA induced neutrophil ($Ly6G^+$ and MPO^+) infiltration and interstitial edema (Fig. 14). The intraperitoneal administration of CYR5099 (10 or 25 mg/kg body weight) resulted in a significant reduction of CFA-induced paw ROS production, neutrophil infiltration, and edema (Fig. 14).

4. Discussion

NOX2, a respiratory burst oxidase, generates $O_2^{\bullet -}$ in activated neutrophils [41,42]. Dysregulation of NOX2 plays a significant role in the development of neutrophil-dominated inflammatory diseases [3]. Therefore, NOX2 is a promising therapeutic target for oxidative stress-related inflammatory diseases. In the present study, we demonstrated that CYR5099, a new small molecule compound derived from benzo[f] indole-4,9-dione, reduces $O_2^{\bullet -}$ production, ROS generation, and CD11b integrin expression in activated human neutrophils via inhibiting NOX2 activity. CYR5099 also showed therapeutic potential against CFA-induced inflammatory arthritis injury.

Neutrophils are essential innate immune cells. Neutrophils generate ROS by NOX2 which can kill pathogen [41–43]. However, large amounts of ROS can cause tissue damage and lead to inflammatory diseases, such as arthritis, psoriasis, and systemic lupus erythematosus [3,44–46]. In this study, we confirmed the anti-inflammatory properties of CYR5099 on reducing oxidative stress caused by activated human neutrophils. CYR5099 does-dependently attenuated $O_2^{\bullet -}$ production and ROS generation in different activators-induced human neutrophils. Previous studies have shown that $O_2^{\bullet -}$ generation in activated neutrophils could be controlled by direct scavenging or regulation of intracellular signaling pathways [47,48]. CYR5099 did not have an inhibitory effect on elastase release in human neutrophils, and it did not display direct $O_2^{\bullet -}$ and free-radical scavenging ability in cell-free assays. These results suggested that CYR5099 selectively inhibited $O_2^{\bullet -}$ production in activated human neutrophils via blocking NOX2 upstream signaling pathway or inhibiting NOX2 activity.

Ca^{2+} is an important second messenger in controlling NOX2 activity [49,50]. Calcium signals in neutrophils are initiated by various membrane-associated receptors, such as G protein-coupled receptors (GPCRs), FcRs, and integrins. GPCR activation triggers intracellular signaling pathways, including conversion of phosphoinositol 4,5-biphosphate to inositol 1,4,5-triphosphate by phospholipase C [49–51]. CYR5099 did not affect intracellular Ca^{2+} mobilization in human neutrophils activated with fMLF, MMK1, f-MMYALF, *m*-3M3FBS, IL-8, LTB_4, and PAF. Thus, the anti-inflammatory effects of CYR5099 were not due to suppression of phospholipase C pathway and intracellular Ca^{2+} mobilization. GPCR activation also stimulates MAPK and Akt phosphorylation, resulting in $p47^{phox}$ or $p67^{phox}$ phosphorylation, $p47^{phox}$-$p67^{phox}$ complex formation, and subsequent activation of NOX2 to induce respiratory burst in neutrophils [52]. CYR5099 did not inhibit the phosphorylation of p38, JNK, and Akt. However, CYR5099 inhibited ERK phosphorylation by 31.6% in fMLF-activated human neutrophils. Previous studies have shown that ROS can induced ERK phosphorylation [53–55]. Therefore, reduction of ERK phosphorylation by CYR5099 may result from its inhibitory effect on ROS formation in activated human neutrophils.

Since CYR5099 did not block NOX2 upstream signaling pathways, we propose that CYR5099 is a direct NOX2 inhibitor. Consistent with our hypothesis, CYR5099 revealed significant inhibitory effects on NOX2-mediated $O_2^{\bullet -}$ generation in PMA-preactivated human neutrophils and SDS-reconstructed subcellular system. $p47^{phox}$ phosphorylation plays a critical role in NOX2 activation [56–58]. The immunofluorescence and immunoblotting assay indicated that CYR5099 did not influence $p47^{phox}$ membrane translocation in activated human neutrophils. Apocynin and DPI, two well-known inhibitors of NOX2 [32], inhibited NOX2-mediated $O_2^{\bullet -}$ generation in activated human neutrophils. ROS can stimulate CD11b expression, which mediates neutrophil adhesion and migration [20,59]. Additionally, angiotensin II-induced T cells tissue homing is ameliorated in $p47^{phox}$-deficient mice [60], suggesting that targeting NOX2 prevents immune cell infiltration. CYR5099 significantly inhibited CD11b expression in fMLF- or PMA-activated human neutrophils. The NOX2 inhibitors, DPI and apocynin, showed the same effects. CYR5099 is a NOX2 inhibitor that functions similar to DPI. The prodrug apocynin requires MPO and H_2O_2 to form an activate NOX2 inhibitor [33–36]. We also noted that apocynin failed to inhibit NOX2-mediated $O_2^{\bullet -}$ generation in SDS-reconstructed subcellular system.

Arthritis is a common health problem resulting from joint inflammation. The pathogenesis of arthritis involves ROS formation, immune cell infiltration, and synovial hyperplasia [61,62]. Previous studies have shown that the severity of arthritis correlates with ROS level and NOX2 overexpression in mice with hypoxic inflammatory arthritis [8]. Excessive ROS generation is also associated with synovial membrane inflammation, and NOX2-mediated ROS production contributes to osteoarthritic joint inflammation and articular cartilage degradation [63]. Our results showed that CYR5099 significantly reduced ROS level, neutrophil infiltration, and edema in CFA-induced paw inflammation in mice. Therefore, targeting NOX2 may have therapeutic potential in arthritis inflammation.

Direct inhibition of NOX2 activity could be dangerous. Chronic granulomatous disease patients, who have defects in $O_2^{\bullet -}$-generating NOX2, suffer from increased susceptibility for bacterial and fungal infections and also other disease conditions such as Crohn's disease and pancolitis [64,65]. Therefore, people should pay attention to the clinical use of NOX2 inhibitors. In this study, an acute inflammatory arthritis mouse model was used to examine the preclinical effect of CYR5099. Our results suggest that CYR5099 may be a lead compound for the development of NOX2 inhibitor to treat neutrophil-dominant acute oxidative inflammatory disorders.

5. Conclusion

In summary, this is the first time to identify a novel small molecule CYR5099 to target NOX2 for restricting neutrophilic inflammation, including $O_2^{\bullet -}$ production, ROS generation, CD11b integrin expression, and cell adhesion. Our *in vivo* study demonstrates that CYR5099 ameliorates neutrophil-mediated inflammatory arthritis. CYR5099 can be a lead compound for the development of NOX2 inhibitor to treat neutrophil-mediated inflammatory diseases.

Conflicts of interest

The authors declare that no competing interests exist.

Acknowledgements

This research was financial supported by the grants from the Ministry of Science and Technology (MOST 108-2320-B-126-001, MOST 106-2320-B-255-003-MY3, MOST 104-2320-B-255-004-MY3, MOST 105-2314-B-182A-012-MY3, MOST 107-2320-B-037-013 and MOST 105-2314-B-182A-137-MY3), Taiwan; Ministry of Education (EMRPD1I0441 and EMRPD1I0501), Taiwan; Chang Gung Memorial Hospital (CMRPG3H0811, CMRPF1F0061~3, CMRPF1G0241~3, CMRPG3E1552, CMRPG3G1601, CMRPG3F6221~3, and BMRP450), Taiwan. The funders had no role in study design, data collection and analysis, decision to publish, or preparation of the manuscript.

Appendix A. Supplementary data

Supplementary data to this article can be found online at https://doi.org/10.1016/j.redox.2019.101273.

References

[1] E. Kolaczkowska, P. Kubes, Neutrophil recruitment and function in health and inflammation, Nat. Rev. Immunol. 13 (3) (2013) 159–175.
[2] B. Amulic, C. Cazalet, G.L. Hayes, K.D. Metzler, A. Zychlinsky, Neutrophil function: from mechanisms to disease, Annu. Rev. Immunol. 30 (2012) 459–489.
[3] L. Glennon-Alty, A.P. Hackett, E.A. Chapman, H.L. Wright, Neutrophils and redox stress in the pathogenesis of autoimmune disease, Free Radic. Biol. Med. 125 (2018) 25–35.
[4] C.C. Winterbourn, A.J. Kettle, M.B. Hampton, Reactive oxygen species and neutrophil function, Annu. Rev. Biochem. 85 (2016) 765–792.
[5] J. El-Benna, M. Hurtado-Nedelec, V. Marzaioli, J.C. Marie, M.A. Gougerot-Pocidalo, P.M. Dang, Priming of the neutrophil respiratory burst: role in host defense and inflammation, Immunol. Rev. 273 (1) (2016) 180–193.
[6] S.A. Belambri, L. Rolas, H. Raad, M. Hurtado-Nedelec, P.M. Dang, J. El-Benna, NADPH oxidase activation in neutrophils: role of the Phosphorylation of its subunits, Eur. J. Clin. Investig. (2018) e12951.
[7] M.H. Hoffmann, H.R. Griffiths, The dual role of ROS in autoimmune and inflammatory diseases: evidence from preclinical models, Free Radic. Biol. Med. 125 (2018) 62–71.
[8] M. Biniecka, M. Connolly, W. Gao, C.T. Ng, E. Balogh, M. Gogarty, L. Santos, E. Murphy, D. Brayden, D.J. Veale, U. Fearon, Redox-mediated angiogenesis in the hypoxic joint of inflammatory arthritis, Arthritis & rheumatology 66 (12) (2014) 3300–3310.
[9] K. Bernard, L. Hecker, T.R. Luckhardt, G. Cheng, V.J. Thannickal, NADPH oxidases in lung health and disease, Antioxidants Redox Signal. 20 (17) (2014) 2838–2853.
[10] K. Hirano, W.S. Chen, A.L. Chueng, A.A. Dunne, T. Seredenina, A. Filippova, S. Ramachandran, A. Bridges, L. Chaudry, G. Pettman, C. Allan, S. Duncan, K.C. Lee, J. Lim, M.T. Ma, A.B. Ong, N.Y. Ye, S. Nasir, S. Mulyanidewi, C.C. Aw, P.P. Oon, S. Liao, D. Li, D.G. Johns, N.D. Miller, C.H. Davies, E.R. Browne, Y. Matsuoka, D.W. Chen, V. Jaquet, A.R. Rutter, Discovery of GSK2795039, a novel small molecule NADPH oxidase 2 inhibitor, Antioxidants Redox Signal. 23 (5) (2015) 358–374.
[11] F.C. Liu, H.P. Yu, C.Y. Lin, A.O. Elzoghby, T.L. Hwang, J.Y. Fang, Use of cilomilast-loaded phosphatiosomes to suppress neutrophilic inflammation for attenuating acute lung injury: the effect of nanovesicular surface charge, J. Nanobiotechnol. 16 (1) (2018) 35.
[12] P.H. Schafer, A. Parton, A.K. Gandhi, L. Capone, M. Adams, L. Wu, J.B. Bartlett, M.A. Loveland, A. Gilhar, Y.F. Cheung, G.S. Baillie, M.D. Houslay, H.W. Man, G.W. Muller, D.I. Stirling, Apremilast, a cAMP phosphodiesterase-4 inhibitor, demonstrates anti-inflammatory activity in vitro and in a model of psoriasis, Br. J. Pharmacol. 159 (4) (2010) 842–855.
[13] M.A. Giembycz, S.K. Field, Roflumilast: first phosphodiesterase 4 inhibitor approved for treatment of COPD, Drug Des. Dev. Ther. 4 (2010) 147–158.
[14] H.L. Wright, R.J. Moots, S.W. Edwards, The multifactorial role of neutrophils in rheumatoid arthritis, Nat. Rev. Rheumatol. 10 (10) (2014) 593–601.
[15] R. Holmdahl, J.C. Lorentzen, S. Lu, P. Olofsson, L. Wester, J. Holmberg, U. Pettersson, Arthritis induced in rats with nonimmunogenic adjuvants as models for rheumatoid arthritis, Immunol. Rev. 184 (2001) 184–202.
[16] M.F. Rossato, C. Hoffmeister, R. Tonello, A.P. de Oliveira Ferreira, J. Ferreira, Anti-inflammatory effects of vitamin E on adjuvant-induced arthritis in rats, Inflammation 38 (2) (2015) 606–615.
[17] S.C. Yang, P.J. Chen, S.H. Chang, Y.T. Weng, F.R. Chang, K.Y. Chang, C.Y. Chen, T.I. Kao, T.L. Hwang, Luteolin attenuates neutrophilic oxidative stress and inflammatory arthritis by inhibiting Raf1 activity, Biochem. Pharmacol. 154 (2018) 384–396.
[18] J.I. Chung, S. Barua, B.H. Choi, B.H. Min, H.C. Han, E.J. Baik, Anti-inflammatory effect of low intensity ultrasound (LIUS) on complete Freund's adjuvant-induced arthritis synovium, Osteoarthr. Cartil. 20 (4) (2012) 314–322.
[19] S.C. Yang, S.H. Chang, P.W. Hsieh, Y.T. Huang, C.M. Ho, Y.F. Tsai, T.L. Hwang, Dipeptide HCH6-1 inhibits neutrophil activation and protects against acute lung injury by blocking FPR1, Free Radic. Biol. Med. 106 (2017) 254–269.
[20] P.J. Chen, Y.L. Wang, L.M. Kuo, C.F. Lin, C.Y. Chen, Y.F. Tsai, J.J. Shen, T.L. Hwang, Honokiol suppresses TNF-alpha-induced neutrophil adhesion on cerebral endothelial cells by disrupting polyubiquitination and degradation of IkappaBalpha, Sci. Rep. 6 (2016) 26554.
[21] T.L. Hwang, H.W. Hung, S.H. Kao, C.M. Teng, C.C. Wu, S.J. Cheng, Soluble guanylyl cyclase activator YC-1 inhibits human neutrophil functions through a cGMP-independent but cAMP-dependent pathway, Mol. Pharmacol. 64 (6) (2003) 1419–1427.
[22] P.C. Braga, M. Dal Sasso, M. Culici, T. Bianchi, L. Bordoni, L. Marabini, Anti-inflammatory activity of thymol: inhibitory effect on the release of human neutrophil elastase, Pharmacology 77 (3) (2006) 130–136.
[23] T.L. Hwang, Y.C. Su, H.L. Chang, Y.L. Leu, P.J. Chung, L.M. Kuo, Y.J. Chang, Suppression of superoxide anion and elastase release by C18 unsaturated fatty acids in human neutrophils, J. Lipid Res. 50 (7) (2009) 1395–1408.
[24] T.L. Hwang, I.A. Aljuffali, C.F. Hung, C.H. Chen, J.Y. Fang, The impact of cationic solid lipid nanoparticles on human neutrophil activation and formation of neutrophil extracellular traps (NETs), Chem. Biol. Interact. 235 (2015) 106–114.
[25] Y.F. Tsai, T.C. Chu, W.Y. Chang, Y.C. Wu, F.R. Chang, S.C. Yang, T.Y. Wu, Y.M. Hsu, C.Y. Chen, S.H. Chang, T.L. Hwang, 6-Hydroxy-5,7-dimethoxy-flavone suppresses the neutrophil respiratory burst via selective PDE4 inhibition to ameliorate acute lung injury, Free Radic. Biol. Med. 106 (2017) 379–392.
[26] H.P. Yu, P.W. Hsieh, Y.J. Chang, P.J. Chung, L.M. Kuo, T.L. Hwang, DSM-RX78, a new phosphodiesterase inhibitor, suppresses superoxide anion production in activated human neutrophils and attenuates hemorrhagic shock-induced lung injury in rats, Biochem. Pharmacol. 78 (8) (2009) 983–992.
[27] F.C. Liu, H.P. Yu, Y.T. Syu, J.Y. Fang, C.F. Lin, S.H. Chang, Y.T. Lee, T.L. Hwang, Honokiol suppresses formyl peptide-induced human neutrophil activation by blocking formyl peptide receptor 1, Sci. Rep. 7 (1) (2017) 6718.
[28] I. Ginis, D.V. Faller, Protection from apoptosis in human neutrophils is determined by the surface of adhesion, Am. J. Physiol. 272 (1 Pt 1) (1997) C295–C309.
[29] A. Kielland, T. Blom, K.S. Nandakumar, R. Holmdahl, R. Blomhoff, H. Carlsen, In vivo imaging of reactive oxygen and nitrogen species in inflammation using the luminescent probe L-012, Free Radic. Biol. Med. 47 (6) (2009) 760–766.
[30] L. Fialkow, Y. Wang, G.P. Downey, Reactive oxygen and nitrogen species as signaling molecules regulating neutrophil function, Free Radic. Biol. Med. 42 (2) (2007) 153–164.
[31] R. Takeya, H. Sumimoto, Regulation of novel superoxide-producing NAD(P)H oxidases, Antioxidants Redox Signal. 8 (9–10) (2006) 1523–1532.
[32] S. Altenhofer, K.A. Radermacher, P.W. Kleikers, K. Wingler, H.H. Schmidt, Evolution of NADPH oxidase inhibitors: selectivity and mechanisms for target engagement, Antioxidants Redox Signal. 23 (5) (2015) 406–427.
[33] M. Mora-Pale, S.J. Kwon, R.J. Linhardt, J.S. Dordick, Trimer hydroxylated quinone derived from apocynin targets cysteine residues of p47phox preventing the activation of human vascular NADPH oxidase, Free Radic. Biol. Med. 52 (5) (2012) 962–969.
[34] J. Stefanska, R. Pawliczak, Apocynin: Molecular Aptitudes, Mediators of Inflammation 2008, (2008), p. 106507.
[35] V.F. Ximenes, M.P. Kanegae, S.R. Rissato, M.S. Galhiane, The oxidation of apocynin catalyzed by myeloperoxidase: proposal for NADPH oxidase inhibition, Arch. Biochem. Biophys. 457 (2) (2007) 134–141.
[36] J.M. Simons, B.A. Hart, T.R. Ip Vai Ching, H. Van Dijk, R.P. Labadie, Metabolic activation of natural phenols into selective oxidative burst agonists by activated human neutrophils, Free Radic. Biol. Med. 8 (3) (1990) 251–258.
[37] D. Gianni, B. Bohl, S.A. Courtneidge, G.M. Bokoch, The involvement of the tyrosine kinase c-Src in the regulation of reactive oxygen species generation mediated by NADPH oxidase-1, Mol. Biol. Cell 19 (7) (2008) 2984–2994.
[38] D. Gianni, N. Taulet, H. Zhang, C. DerMardirossian, J. Kister, L. Martinez, W.R. Roush, S.J. Brown, G.M. Bokoch, H. Rosen, A novel and specific NADPH oxidase-1 (Nox1) small-molecule inhibitor blocks the formation of functional invadopodia in human colon cancer cells, ACS Chem. Biol. 5 (10) (2010) 981–993.
[39] P.J. Chen, I.L. Ko, C.L. Lee, H.C. Hu, F.R. Chang, Y.C. Wu, Y.L. Leu, C.C. Wu, C.Y. Lin, C.Y. Pan, Y.F. Tsai, T.L. Hwang, Targeting allosteric site of AKT by 5,7-dimethoxy-1,4-phenanthrenequinone suppresses neutrophilic inflammation, EBioMedicine 40 (2019) 528–540.
[40] L.C. Tajra, X. Martin, J. Margonari, N. Blanc-Brunat, M. Ishibashi, G. Vivier, J.P. Steghens, H. Kawashima, M. Miyasaka, J.M. Dubernard, J.P. Revillard, Antibody-induced modulation of the leukocyte CD11b integrin prevents mild but not major renal ischaemic injury, Nephrol. Dial. Transplant. 15 (10) (2000) 1556–1561.
[41] B.M. Babior, J.D. Lambeth, W. Nauseef, The neutrophil NADPH oxidase, Arch. Biochem. Biophys. 397 (2) (2002) 342–344.
[42] J. El-Benna, P.M. Dang, M.A. Gougerot-Pocidalo, J.C. Marie, F. Braut-Boucher, p47phox, the phagocyte NADPH oxidase/NOX2 organizer: structure, phosphorylation and implication in diseases, Exp. Mol. Med. 41 (4) (2009) 217–225.
[43] B.H. Segal, M.J. Grimm, A.N. Khan, W. Han, T.S. Blackwell, Regulation of innate immunity by NADPH oxidase, Free Radic. Biol. Med. 53 (1) (2012) 72–80.
[44] M. Mittal, M.R. Siddiqui, K. Tran, S.P. Reddy, A.B. Malik, Reactive oxygen species in inflammation and tissue injury, Antioxidants Redox Signal. 20 (7) (2014) 1126–1167.
[45] J. El Benna, G. Hayem, P.M. Dang, M. Fay, S. Chollet-Martin, C. Elbim, O. Meyer, M.A. Gougerot-Pocidalo, NADPH oxidase priming and p47phox phosphorylation in neutrophils from synovial fluid of patients with rheumatoid arthritis and spondylarthropathy, Inflammation 26 (6) (2002) 273–278.
[46] F.J. Bloomfield, M.M. Young, Enhanced chemiluminescence production by phagocytosing neutrophils in psoriasis, Inflammation 12 (2) (1988) 153–159.
[47] N. Kitaoka, G. Liu, N. Masuoka, K. Yamashita, M. Manabe, H. Kodama, Effect of sulfur amino acids on stimulus-induced superoxide generation and translocation of p47phox and p67phox to cell membrane in human neutrophils and the scavenging of free radical, Clinica chimica acta, Int. J. Clin. Chem. 353 (1–2) (2005) 109–116.
[48] S.C. Yang, P.J. Chung, C.M. Ho, C.Y. Kuo, M.F. Hung, Y.T. Huang, W.Y. Chang, Y.W. Chang, K.H. Chan, T.L. Hwang, Propofol inhibits superoxide production, elastase release, and chemotaxis in formyl peptide-activated human neutrophils by blocking formyl peptide receptor 1, J. Immunol. 190 (12) (2013) 6511–6519.
[49] I. Migeotte, D. Communi, M. Parmentier, Formyl peptide receptors: a promiscuous subfamily of G protein-coupled receptors controlling immune responses, Cytokine Growth Factor Rev. 17 (6) (2006) 501–519.
[50] M.C. Lavigne, P.M. Murphy, T.L. Leto, J.L. Gao, The N-formylpeptide receptor (FPR) and a second G(i)-coupled receptor mediate fMet-Leu-Phe-stimulated activation of NADPH oxidase in murine neutrophils, Cell. Immunol. 218 (1–2) (2002) 7–12.
[51] M.D. Salmon, J. Ahluwalia, Pharmacology of receptor operated calcium entry in human neutrophils, Int. Immunopharmacol. 11 (2) (2011) 145–148.
[52] Y. Lin, R. Jia, Y. Liu, Y. Gao, X. Zeng, J. Kou, B. Yu, Diosgenin inhibits superoxide generation in FMLP-activated mouse neutrophils via multiple pathways, Free Radic. Res. 48 (12) (2014) 1485–1493.
[53] K. Ke, O.J. Sul, E.K. Choi, A.M. Safdar, E.S. Kim, H.S. Choi, Reactive oxygen species induce the association of SHP-1 with c-Src and the oxidation of both to enhance osteoclast survival, Am. J. Physiol. Endocrinol. Metab. 307 (1) (2014) 67–70.
[54] R. Bhattacharyya A Fau - Chattopadhyay, S. Chattopadhyay R Fau - Mitra, S.E. Mitra S Fau - Crowe, S.E. Crowe, Oxidative stress: an essential factor in the

pathogenesis of gastrointestinal mucosal diseases, Physiol. Rev. 94 (2) (2014) 329–354.
[55] K. Traore, R. Sharma, R.K. Thimmulappa, W.H. Watson, S. Biswal, M.A. Trush, Redox-regulation of Erk1/2-directed phosphatase by reactive oxygen species: role in signaling TPA-induced growth arrest in ML-1 cells, J. Cell. Physiol. 216 (1) (2008) 276–285.
[56] W. Liu, H. Wu, L. Chen, Y. Wen, X. Kong, W.Q. Gao, Park7 interacts with p47(phox) to direct NADPH oxidase-dependent ROS production and protect against sepsis, Cell Res. 25 (6) (2015) 691–706.
[57] A. Aljada, H. Ghanim, P. Dandona, Translocation of p47phox and activation of NADPH oxidase in mononuclear cells, Methods Mol. Biol. 196 (2002) 99–103.
[58] J. Renwick, E.P. Reeves, F.B. Wientjes, K. Kavanagh, Translocation of proteins homologous to human neutrophil p47phox and p67phox to the cell membrane in activated hemocytes of Galleria mellonella, Dev. Comp. Immunol. 31 (4) (2007) 347–359.
[59] G. Svineng, O. Ravuri C Fau - Rikardsen, N.-E. Rikardsen O Fau - Huseby, J.-O. Huseby Ne Fau - Winberg, J.O. Winberg, The role of reactive oxygen species in integrin and matrix metalloproteinase expression and function, Connect. Tissue Res. 49 (3) (2008) 197–202.
[60] T.J. Guzik, N.E. Hoch, K.A. Brown, L.A. McCann, A. Rahman, S. Dikalov, J. Goronzy, C. Weyand, D.G. Harrison, Role of the T cell in the genesis of angiotensin II induced hypertension and vascular dysfunction, J. Exp. Med. 204 (10) (2007) 2449–2460.
[61] C.O. Bingham 3rd, The pathogenesis of rheumatoid arthritis: pivotal cytokines involved in bone degradation and inflammation, J. Rheumatol. Suppl. 65 (2002) 3–9.
[62] P. Miossec, Update on interleukin-17: a role in the pathogenesis of inflammatory arthritis and implication for clinical practice, RMD open 3 (1) (2017) e000284.
[63] D. Clavijo-Cornejo, K. Martinez-Flores, K. Silva-Luna, G.A. Martinez-Nava, J. Fernandez-Torres, Y. Zamudio-Cuevas, M. Guadalupe Santamaria-Olmedo, J. Granados-Montiel, C. Pineda, A. Lopez-Reyes, The Overexpression of NALP3 Inflammasome in Knee Osteoarthritis Is Associated with Synovial Membrane Prolidase and NADPH Oxidase 2, Oxidative Medicine and Cellular Longevity 2016, (2016), p. 1472567.
[64] G. Aviello, U.G. Knaus, ROS in gastrointestinal inflammation: rescue or Sabotage? Br. J. Pharmacol. 174 (12) (2017) 1704–1718.
[65] S. O'Neill, J. Brault, M.J. Stasia, U.G. Knaus, Genetic disorders coupled to ROS deficiency, Redox Biol. 6 (2015) 135–156.